

# Dioxygenases catalyze the O-demethylation steps of morphine biosynthesis in opium poppy

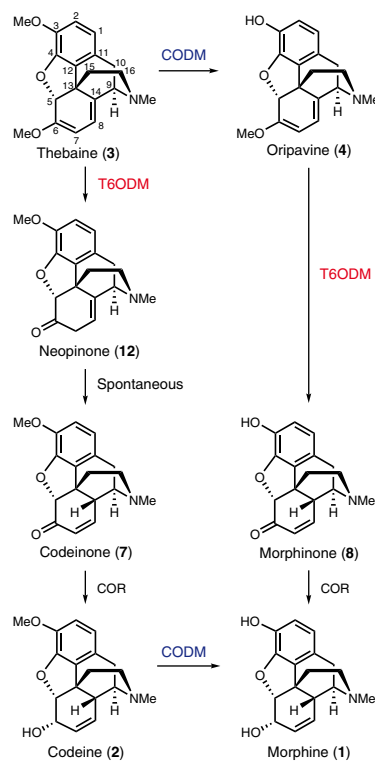
Jillian M Hagel & Peter J Facchini\*

**Two previously undetected enzymes involved in morphine biosynthesis and unique among plants to opium poppy have been identified as non-heme dioxygenases, in contrast to the functionally analogous cytochrome P450s found in mammals. We used functional genomics to isolate thebaïne 6-O-demethylase (T6ODM) and codeine O-demethylase (CODM), the only known 2-oxoglutarate/Fe(II)-dependent dioxygenases that catalyze O-demethylation. Virus-induced gene silencing of T6ODM and CODM in opium poppy efficiently blocked metabolism at thebaïne and codeine, respectively.**

The medicinal properties of opium poppy (*Papaver somniferum* L.) have been recognized since the dawn of civilization. The licit cultivation of the plant remains the sole commercial source for several widely used pharmaceuticals, including morphine (1), codeine (2) and semisynthetic derivatives such as oxycodone. The more extensive illicit cultivation of opium poppy for the production of heroin (O,O-diacetylmorphine) continues to have profound and negative global consequences. The biosynthesis of morphine and related alkaloids in opium poppy occurs via a multistep pathway beginning with the amino acid tyrosine<sup>1</sup> (Supplementary Fig. 1). Corresponding genes encoding many of the enzymes involved in morphine biosynthesis have been isolated. However, enzymes responsible for O-demethylation at positions 6 and 3, which represent two of the three steps in the conversion of thebaïne (3) to morphine (Scheme 1), have never been detected. In humans, the 3-O-demethylation of thebaïne and codeine is catalyzed by CYP2D6 (refs. 2,3), and cytochrome P450s have been suggested as the enzymes responsible for the corresponding reactions in opium poppy<sup>4,5</sup>.

Avoiding the presupposition that the analogous plant enzymes are also cytochrome P450s, we used differential gene expression analysis of a mutant opium poppy chemotype to identify a candidate complementary DNA encoding thebaïne 6-O-demethylase. Natural and induced mutants of opium poppy including the *top1* variety<sup>6</sup> have been reported to accumulate high levels of thebaïne and oripavine (4), but not morphine or codeine<sup>7,8</sup>. The development of the *top1* variety using chemical mutagenesis was a major breakthrough for the opium poppy industry in Australia, as it allowed the efficient production of thebaïne from morphine-free plants. Thebaïne is the natural precursor used in the synthesis of several pharmaceuticals including oxycodone, naltrexone, naloxone and buprenorphine. Although the metabolic block in *top1* was suggested to result from a defect in the enzyme catalyzing the 6-O-demethylation of thebaïne and oripavine, the biochemical basis for the phenotype was not determined<sup>6</sup>. Previously, we described an opium poppy variety (designated “T”) with a *top1* alkaloid profile<sup>8</sup>. The high-thebaïne, high-oripavine, morphine- and codeine-free phenotype in T displayed Mendelian inheritance as a single, recessive locus (Supplementary Table 1). The stem transcriptome of T was then independently compared with the stem transcriptomes of three morphine-accumulating varieties (L, 11 and 40) using a cDNA

fragment-based 23,000-element microarray (Supplementary Figs. 2 and 3). Integration of all three pair-wise comparisons revealed eight candidate cDNAs exhibiting transcript levels that were lower in T compared with at least two of the high-morphine varieties. Among these, only one encoding a putative 2-oxoglutarate/Fe(II)-dependent dioxygenase (DIOX1) showed transcript levels that were lower in T compared with L, 11 and 40. This was noteworthy owing to the increased thebaïne and reduced morphine content of opium poppy plants treated with the acylcyclohexanediones prohexadione



**Scheme 1 | Morphinan alkaloid biosynthesis in opium poppy, showing two routes from thebaïne to morphine.** O-Demethylation at position 6 is catalyzed by T6ODM, whereas O-demethylation at position 3 is catalyzed by CODM. Thebaïne can undergo O-demethylation at position 6 or position 3 to yield neopinone (12) or oripavine, respectively. Neopinone spontaneously rearranges to the more stable codeinone in aqueous solution over a wide pH range<sup>25</sup>—a process that is expedited under physiological conditions by the reduction of codeinone to codeine by codeinone reductase (COR). Codeine is demethylated by CODM to produce morphine. Demethylation of oripavine by T6ODM yields morphinone, which is reduced to morphine by COR. The opium poppy variety T used in this study is blocked at T6ODM, and accumulates thebaïne and oripavine rather than morphine and codeine.

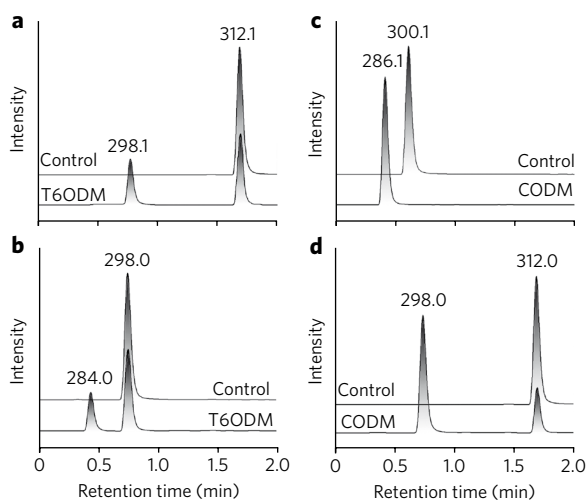


**Figure 1 | Extracted ion chromatograms showing the substrates and products of T6ODM and CODM enzyme assays.** In each panel, the upper (control) extracted ion chromatogram corresponds to an assay performed with boiled enzyme, whereas the lower (T6ODM or CODM) extracted ion chromatogram shows an assay performed with native enzyme. Reaction products were unambiguously identified using collision-induced dissociation analysis, and the resulting daughter ion mass spectra are shown in **Supplementary Figure 7**. (a) T6ODM assay with thebeaine as the substrate ( $m/z$  312.1) and codeinone as the product ( $m/z$  298.1). Neopinone, which is unstable and spontaneously rearranges to codeinone in aqueous solutions<sup>25</sup>, was not detected. (b) T6ODM assay with oripavine as the substrate ( $m/z$  298.0) and morphinone as the product ( $m/z$  284.0). (c) CODM assay with codeine as the substrate ( $m/z$  300.1) and morphine as the product ( $m/z$  286.1). (d) CODM assay with thebeaine as the substrate ( $m/z$  312.1) and oripavine as the product ( $m/z$  298.0). T6ODM assays were analyzed after 1 h to minimize the spontaneous formation of codeinone or morphinone adducts. CODM assays were stopped after 4 h.

calcium (5) and trinexapac-ethyl (6)<sup>9</sup>, which inhibit dioxygenases involved in the biosynthesis of gibberellin hormones.

We used the DIOX1 amino acid sequence to query our opium poppy expressed sequence tag database, which led to the identification of two highly conserved homologs (designated DIOX2 and DIOX3) (**Supplementary Methods**). A phylogenetic tree comparing several characterized and putative plant 2-oxoglutarate/Fe(II)-dependent dioxygenases placed these DIOX proteins into a distinct clade (**Supplementary Fig. 4**). Each DIOX protein had the canonical HXDX<sub>2</sub>H catalytic triad required for coordinating Fe(II), and a YX<sub>2</sub>RXS motif implicated in 2-oxoglutarate binding<sup>10</sup> (**Supplementary Fig. 5**). Recombinant His<sub>6</sub>-tagged proteins produced in *Escherichia coli* (**Supplementary Table 2**) and purified by cobalt-affinity chromatography (**Supplementary Fig. 6**) were tested for 2-oxoglutarate/Fe(II)-dependent O-demethylase activity using thebeaine, oripavine or codeine as substrates. Assays consisted of Fe(II) and ascorbate as cofactors, 2-oxoglutarate and a morphinan alkaloid as substrates, and a recombinant DIOX enzyme. After incubation at 30 °C for up to 4 h, the reactions were quenched and analyzed using liquid chromatography–tandem mass spectrometry (**Fig. 1** and **Supplementary Fig. 7**).

DIOX1 catalyzed the 6-O-demethylation of thebeaine and oripavine, yielding codeinone (**Fig. 1a**) and morphinone (**Fig. 1b**), respectively. Conversely, DIOX3 catalyzed the 3-O-demethylation of codeine (**Fig. 1c**) and thebeaine (**Fig. 1d**), yielding morphine and oripavine, respectively. As such, DIOX1 was renamed thebeaine 6-O-demethylase (T6ODM) and DIOX3 was renamed codeine O-demethylase (CODM). The enzymatic synthesis of codeinone (7) and morphinone (8) by T6ODM was accompanied by the spontaneous formation of several higher molecular weight adducts. The general instability of codeinone and morphinone in aqueous solution<sup>11,12</sup> and their reactivity with thiol-containing agents such as 2-mercaptoethanol<sup>13</sup> in the assay mixture is well documented. DIOX2 did not accept thebeaine, oripavine or codeine as substrates. Notably, CODM also catalyzed the regiospecific 3-O-demethylation of the protoberberine alkaloid (S)-scoulerine (9) (**Supplementary Figs. 8 and 9**). Although morphinan and protoberberine alkaloids have different skeletal structures, both are members of the large and diverse group of benzyloisoquinoline alkaloids (BIAs). The substrate specificity of T6ODM, CODM and DIOX2 were further examined using an assay based on the O-demethylation–coupled decarboxylation of [1-<sup>14</sup>C]2-oxoglutarate<sup>14</sup>, which showed that other structural categories of BIAs having O-linked methyl groups were not accepted as substrates (**Supplementary Fig. 8**). Using the same assay, recombinant T6ODM produced  $K_m$  values for thebeaine and oripavine of  $20 \pm 7$  and  $15 \pm 3$   $\mu$ M, respectively, whereas CODM exhibited  $K_m$  values of  $21 \pm 8$  and  $42 \pm 8$   $\mu$ M for codeine and thebeaine, respectively (**Supplementary Table 3** and **Supplementary Fig. 10**). The catalytic efficiency of CODM was lower with thebeaine ( $k_{cat}/K_m = 235$  s<sup>-1</sup> M<sup>-1</sup>) than with codeine ( $k_{cat}/K_m = 785$  s<sup>-1</sup> M<sup>-1</sup>) as the substrate. These results suggest the pathway through codeinone as the preferred route in morphine biosynthesis (**Scheme 1**)<sup>15,16</sup>. The  $K_m$  values of T6ODM and CODM for 2-oxoglutarate were similar to those described for other plant 2-oxoglutarate/Fe(II)-dependent dioxygenases<sup>17</sup>. T6ODM, DIOX2 and CODM represent the first known O-demethylases in the 2-oxoglutarate/Fe(II)-dependent dioxygenase family<sup>18,19</sup>. We have deposited the corresponding gene sequences in the Entrez Gene database under accession numbers GQ500139 (T6ODM), GQ500140 (DIOX2) and GQ500141 (CODM).

Related plant enzymes such as anthocyanidin synthase, flavonol synthase and flavanone 3 $\beta$ -hydroxylase catalyze ring hydroxylation, with all but the latter leading to the introduction of double bonds.

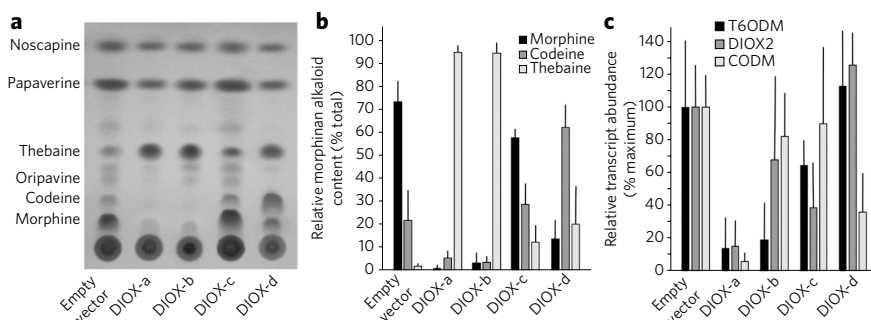


**Figure 2 | Virus-induced gene silencing analysis.** Opium poppy seedlings were infiltrated with *Agrobacterium tumefaciens* strain GV3101 harboring pTRV1 and one of five different pTRV2 constructs. DIOX-a contained a highly conserved sequence from the coding regions of T6ODM, DIOX2 and CODM. DIOX-b, DIOX-c and DIOX-d contained gene-specific sequences from the 3' UTRs of T6ODM, DIOX2 and CODM, respectively. pTRV2 was used as the empty vector. (a) TLC of latex extracted in methanol. The  $R_f$  positions of authentic alkaloid standards are indicated in the left margin. (b) HPLC of latex extracts. Each bar represents the mean  $\pm$  s.d. for triplicate samples from 3 independent plants. (c) Real-time quantitative PCR analysis of T6ODM, DIOX2 and CODM gene transcript levels in stem samples from plants analyzed by TLC and HPLC. Each bar represents the mean  $\pm$  s.d. of 27 values (that is, 3 technical replicates on RNA samples extracted from each of 3 stem segments taken from each of 3 individual plants).

The hydroxylation of alkyl moieties is the most common reaction catalyzed by 2-oxoglutarate/Fe(II)-dependent dioxygenases. The N-demethylation of histones and nucleic acids proceeds via hydroxylation of the N-methyl moiety followed by formaldehyde elimination<sup>20</sup>. Similarly, we propose that T6ODM and CODM catalyze O-demethylation by hydroxylation of the O-methyl group. The formation of formaldehyde was confirmed using the Nash reaction<sup>21</sup> (Supplementary Fig. 11). Notably, acylcyclohexanediones did not inhibit enzyme activity *in vitro*, suggesting an indirect mode of action for the reduced metabolic flux past thebaine in plants treated with these compounds.

The metabolic functions of T6ODM and CODM were investigated *in planta* using virus-induced gene silencing (VIGS). Fragments of T6ODM, DIOX2 and CODM cDNAs (Supplementary Fig. 12) were introduced systemically into opium poppy using the tobacco rattle virus (TRV) as a vector. One pTRV2-based construct (DIOX-a) contained a conserved sequence from the coding region of T6ODM and was designed to silence all three genes simultaneously. In contrast, DIOX-b, DIOX-c and DIOX-d contained unique sequences from the 3' untranslated regions (UTRs) of the T6ODM, DIOX2 and CODM genes, respectively, and were designed to silence each gene individually. Emerging first leaves of 2-week-old to 3-week-old opium poppy seedlings were infiltrated with *Agrobacterium tumefaciens* harboring one of these four constructs, or the empty vector (pTRV2) as a control. The alkaloid content of the latex and the relative abundance of T6ODM, DIOX2 and CODM gene transcripts in the stem of infected plants were determined immediately before the onset of flowering (Fig. 2). The opium poppy variety used for the VIGS experiments accumulates an abundance of morphine, lower levels of codeine and thebaine, trace quantities of oripavine, and substantial amounts of noscapine (10) and papaverine (11). Plants treated with the empty pTRV2 vector displayed a wild-type alkaloid profile (Fig. 2a,b). In contrast, the DIOX-a and T6ODM gene-specific DIOX-b constructs resulted in a near-complete metabolic block at thebaine. The CODM gene-specific DIOX-d construct caused a substantial increase in codeine accumulation compared with morphine. Oripavine was not detected in plants treated with the DIOX-a or DIOX-d constructs as a result of silencing CODM, since the gene product converts thebaine to oripavine. The silencing of DIOX2 had no detectable effect on alkaloid content. Real-time quantitative PCR confirmed the gene-specific silencing of T6ODM, DIOX2 and/or CODM (Fig. 2c). Only partial transcript reduction was achieved for DIOX2, perhaps owing to the use of a relatively short 3' UTR fragment in the DIOX-c construct (Supplementary Fig. 12). The catalytic properties of T6ODM and CODM with respect to morphine biosynthesis were fully corroborated *in planta* using VIGS. The physiological relevance of the scoulerine 3-O-demethylase activity of each enzyme must still be determined.

Approximately 2,500 BIA structures occur naturally in members of several plant families, yet only opium poppy produces morphine and codeine. The recruitment of T6ODM and CODM from an ancestral 2-oxoglutarate/Fe(II)-dependent dioxygenase, perhaps one originally involved in protoberberine alkaloid metabolism, was a milestone evolutionary event that continues to have profound consequences, both positive and negative, for humankind. The discovery of these new enzymes could have major industrial, pharmaceutical and socioeconomic implications. Most of the licit morphine recovered from opium poppy is synthetically 3-O-methylated to yield codeine<sup>22</sup>, which is a more versatile analgesic and cough suppressant. The development of an opium poppy variety blocked at CODM would allow the direct recovery of codeine from the plant and prevent the formation of morphine, which would preclude the illicit synthesis of heroin. The extensive deployment of the *top1* variety in Australia underscores the growing demand for semisynthetic opiates, especially oxycodone, and demonstrates the commercial potential for opium poppy varieties with altered

morphinan alkaloid profiles. Our discovery of T6ODM provides a biochemical basis for the *top1* and T phenotype<sup>6</sup> and a tool to identify the genetic mechanism responsible for the specific silencing of the T6ODM gene (Supplementary Fig. 13) in opium poppy varieties blocked at thebaine. Recently, the feasibility of reconstituting BIA metabolism in yeast (*Saccharomyces cerevisiae*) has also been demonstrated<sup>23,24</sup>. Genes encoding T6ODM and CODM are essential for the production of codeine and morphine in scalable microbial systems, which could provide an alternative to conventional agriculture with respect to production cost and the regulation of controlled substances.

Received 8 September 2009; accepted 29 December 2009; published online 14 March 2010

## References

1. Ziegler, J. & Facchini, P.J. *Annu. Rev. Plant Biol.* **59**, 735–769 (2008).
2. Zhu, W. *Med. Sci. Monit.* **14**, SC15–SC18 (2008).
3. Grobe, N. *et al. J. Biol. Chem.* **284**, 24425–24431 (2009).
4. Unterlinner, B., Lenz, R. & Kutchan, T.M. *Plant J.* **18**, 465–475 (1999).
5. Grothe, T., Lenz, R. & Kutchan, T.M. *J. Biol. Chem.* **276**, 30717–30723 (2001).
6. Millgate, A.G. *et al. Nature* **431**, 413–414 (2004).
7. Nyman, U. *Hereditas* **89**, 43–50 (1978).
8. Hagel, J.M., Weljie, A.M., Vogel, H.J. & Facchini, P.J. *Plant Physiol.* **147**, 1805–1821 (2008).
9. Cotterill, P. Method of altering the alkaloid composition in poppy plants. International patent WO/2005/107436 (2005).
10. Wilmoth, R.C. *et al. Structure* **10**, 93–103 (2002).
11. Lister, D.L., Kanungo, G., Rathbone, D.A. & Bruce, N.C. *FEMS Microbiol. Lett.* **181**, 137–144 (1999).
12. Craig, D.H., Moody, P.C.E., Bruce, N.C. & Scrutton, N.S. *Biochemistry* **37**, 7598–7607 (1998).
13. Ishida, T., Yano, M. & Toki, S. *Drug Metab. Dispos.* **19**, 895–899 (1991).
14. Tiainen, P., Myllyharju, J. & Koivunen, P. *J. Biol. Chem.* **280**, 1142–1148 (2005).
15. Nielsen, B., Røe, J. & Brochmann-Hanssen, E. *Planta Med.* **48**, 205–206 (1983).
16. Brochmann-Hanssen, E. *Planta Med.* **50**, 343–345 (1984).
17. De Carolis, E. & De Luca, V. *Phytochemistry* **36**, 1093–1107 (1994).
18. Hausinger, R.P. *Crit. Rev. Biochem. Mol. Biol.* **39**, 21–68 (2004).
19. Clifton, I.J. *et al. J. Inorg. Biochem.* **100**, 644–669 (2006).
20. Loenarz, C. & Schofield, C.J. *Nat. Chem. Biol.* **4**, 152–156 (2008).
21. Rapoport, R., Hanukoglu, I. & Sklan, D. *Anal. Biochem.* **218**, 309–313 (1994).
22. International Narcotics Control Board. Narcotic drugs: estimated world requirements for 2007; statistics for 2005 (E/INCB/2006/2). (United Nations Publications, 2006).
23. Hawkins, K.M. & Smolke, C.D. *Nat. Chem. Biol.* **4**, 564–573 (2008).
24. Minami, H. *et al. Proc. Natl. Acad. Sci. USA* **105**, 7393–7398 (2008).
25. Parker, H.L., Blaschke, G. & Rapoport, H. *J. Am. Chem. Soc.* **94**, 1276–1282 (1972).

## Acknowledgments

We are grateful to D. Kumar (Yale University) for the pTRV1 and pTRV2 vectors, V. Irish (Yale University) for the pTRV2-PapPDS construct, the Canadian National Research Council Plant Biotechnology Institute for hosting our sequence data on their FIESTA2 annotation platform, and Sanofi-Aventis for the gift of the opium poppy varieties and the alkaloid standards used in this work. We also thank K. Zulak, R. Bourgault and J. Ziegler for technical assistance with cDNA library construction, microarray preparation and mass spectrometry, respectively. J.M.H. is the recipient of an Alberta Ingenuity Graduate Scholarship. Funding for this work was provided through a Discovery Grant from the Natural Sciences and Engineering Research Council of Canada and a Canada Research Chair in Plant Metabolic Processes Biotechnology, both awarded to P.J.F.

## Author contributions

J.M.H. and P.J.F. contributed equally to all aspects of the experimental design and execution, and the preparation of the manuscript.

## Competing financial interests

The authors declare no competing financial interests.

## Additional information

Supplementary information and chemical compound information is available online at <http://www.nature.com/naturechemicalbiology/>. Reprints and permissions information is available online at <http://npg.nature.com/reprintsandpermissions/>. Correspondence and requests for materials should be addressed to P.J.F.

## Methods

### Plant material

Three commercial, high-morphine varieties (i.e. L, 11 and 40) of opium poppy (*Papaver somniferum*) and a mutant variety (i.e. T) that accumulates high levels of thebaine and oripavine, but lacks morphine and codeine<sup>8</sup>, were cultivated in a growth chamber (Convion, Winnipeg, Canada) at 20°C/18°C (light/dark) under high-intensity metal halide lights with a photoperiod of 16 h. Plant materials for gene expression and/or alkaloid analysis was harvested one day before the onset of flowering and stored at -80°C until further analysis. For virus-induced gene silencing (VIGS) experiments, the opium poppy variety Bea's Choice was cultivated under greenhouse conditions.

### Chemicals

Morphine and codeine were gifts from Sanofi-Aventis (Paris, France; <http://en.sanofi-aventis.com>). Thebaine and oripavine were isolated from the latex of opium poppy variety T. Methanol extracts of T latex were concentrated under reduced pressure and spotted on thin layer chromatography (TLC) Silica gel 60 F<sub>254</sub> plates (Merck, Whitehouse Station, NJ; <http://www.merck.com>). TLC was performed as described previously<sup>6</sup> and alkaloids were visualized under UV illumination at 254 nm. Silica was scraped off the plates from regions corresponding to the R<sub>f</sub> values of authentic thebaine and oripavine and extracted three times with methanol. Pooled methanol extracts were concentrated under reduced pressure. The purity and identity of thebaine and oripavine were confirmed by electron-impact-mass spectrometry (EI-MS). The EI mass spectra were in agreement with those reported previously<sup>15,26</sup>. Noscapine and papaverine were purchased from Sigma-Aldrich (St. Louis, MO; <http://www.sigmaaldrich.com>). Other alkaloids were available as described previously<sup>27,28</sup>. [1-<sup>14</sup>C]2-Oxoglutarate was purchased from American Radiolabeled Chemicals (St. Louis, MO; <http://www.arcincusa.com>). All other chemicals were purchased from Sigma-Aldrich.

### Genetic inheritance

To determine the mode of inheritance underlying the alkaloid phenotype of variety T (i.e. high-thebaine/oripavine, morphine/codeine-free) reciprocal crosses were generated between T and the high-morphine cultivars 11 and 40. Flower buds were dissected one day prior to anthesis, immature stamens were excised and stigmas were pollinated with pollen from the appropriate variety or cross. Pollinated flowers were covered for 1-2 days to allow the development of seed capsules free from contaminating pollen. F<sub>1</sub> plants were either self-pollinated for the production of F<sub>2</sub> seed, or backcrossed with P<sub>1</sub> plants. The alkaloid phenotypes of individual F<sub>2</sub> and backcrossed plants were qualitatively scored as described in the metabolite profiling section. The frequency of plants from each cross that displayed the high-thebaine/oripavine, morphine/codeine-free phenotype (i.e. %T) is shown in Supplementary Table 1.



## Phylogenetic analysis

Phylogeny (Supplementary Fig. 4) and amino acid alignments (Supplementary Fig. 5) were performed using ClustalX<sup>29</sup>, and phylogenetic data were displayed using TREEVIEW<sup>30</sup>. Species and associated GenBank accession numbers are as follows: *Anisodus acutangulus* hyoscyamine 6 $\beta$ -hydroxylase AaH6H (ABM74185); *Arabidopsis thaliana* senescence-related gene 1 AtSRG1 (NP\_173145); *Arabidopsis thaliana* 4-hydroxyphenylpyruvate dioxygenase At4HPPD (AAB58404); *Arabidopsis thaliana* anthocyanidin synthase AtAS (Q96323); *Atropa belladonna* hyoscyamine 6 $\beta$ -hydroxylase AbH6H (BAA78340); *Catharanthus roseus* desacetoxylvindoline 4-hydroxylase CrD4H (AAC49827); *Citrus unshiu* flavanol synthase CuFS (BAA36554); *Coptis japonica* norcoclaurine synthase-1 CjNCS (A2A1A0) *Cucurbita maxima* gibberellin 7-oxidase CmG70 (AAB64346); *Cucurbita maxima* gibberellin 20-oxidase CmG200 (AAB64345); *Citrus unshiu* flavanol synthase CuFS (BAA36554); *Papaver somniferum* thebaine 6-O-demethylase PsT6ODM (GQ500139); *Papaver somniferum* codeine O-demethylase PsCODM (GQ500141); *Papaver somniferum* PsDIOX2 (GQ500140); *Petunia hybrida* flavanone 3 $\beta$ -hydroxylase PhF3H (AAC49929); *Populus trichocarpa* Pt\_dioxygenase-like (XP\_002300453); *Ricinus communis* Rc\_dioxygenase-like (EEF42734); *Solanum lycopersicum* ACC oxidase SLACCO (P24157); *Vitis vinifera* Vv\_dioxygenase-like (CA070478); *Hyoscyamus niger* hyoscyamine 6 $\beta$ -hydroxylase HnH6H (AAA3338); *Zea mays* flavonol synthase/flavanone 3-hydroxylase ZmFS/F3H (ACG44904).

## Microarray construction

A custom-built opium poppy microarray was constructed based on expressed sequence tags (ESTs) derived from elicited cell culture<sup>31</sup> and stem cDNA libraries. A total of 22,752 spots were printed corresponding to 12,768 ESTs from cell culture and 9,984 ESTs from stem, which represented a total of 19,185 genetic elements and 14,355 unigenes. To construct the stem cDNA library, 10 cm of stem immediately below the flower buds of opium poppy variety L were harvested one day prior to anthesis. Total RNA isolation was performed as described previously<sup>32</sup> and poly(A)<sup>+</sup> RNA was selected by oligo(dT)-cellulose chromatography. A unidirectional cDNA library was constructed in  $\lambda$ Uni-ZAPII XR, according to the instructions of the manufacturer (Stratagene, Santa Clara, CA; <http://www.stratagene.com>). An amplified cDNA library derived from approximately  $1 \times 10^7$  primary plaque-forming units was mass excised, and individual bacterial colonies were randomly isolated and cultured in 96-well microtiter plates. Plasmid DNA was prepared using the TempliPhi amplification kit (GE Healthcare Life Sciences, Piscataway, NJ; <http://www.gelifesciences.com>) and sequenced from the 5'-end using a 3730xl capillary electrophoresis DNA analyzer (Applied Biosystems, Foster City, CA; <http://www.appliedbiosystems.com>). Stem expressed sequence tags (ESTs) were analyzed as described previously<sup>27,31</sup>. Sequenced cDNAs from elicited cell culture and stem libraries were

amplified from pBluescript SK<sup>+</sup> using T3 and T7 primers in 0.2 ml capacity 96-well PCR plates (Corning, Corning, NY; <http://www.corning.com>). Agarose gel electrophoresis was used to ensure that each reaction produced sufficient amplicon abundance. PCR products were purified using Montage PCR<sub>96</sub> plates (Millipore, Billerica, MA; <http://www.millipore.com>), recovered in 50 µl of water, transferred to polypropylene V-bottom 96-well plates (Corning), lyophilized to dryness, resuspended in 6 µl 3 x SSC buffer, and arrayed into 384-well polypropylene V-bottom plates (Axygen; Union City, CA; <http://www.axxygen.com>) for printing (Microarray and Proteomics Facility, University of Alberta. Individual spots were printed using a BioMek FX (Beckman-Coulter, Fullerton, CA; <http://www.beckman.com>) onto SuperAmine Substrate (Arralt, Sunnyvale, CA; <http://www.arrayit.com>) slides.

### **Microarray hybridization and analysis**

RNA from opium poppy stem tissue was isolated using a previously described protocol<sup>33</sup> involving guanidinium thiocyanate-based extraction and cesium chloride-based density centrifugation. High quality RNA (100 µg) was reverse transcribed using BD PowerScript reverse transcriptase (BD Biosciences, Franklin Lakes, NJ; <http://www.bdbiosciences.com>) and labeled with Cy3- or Cy5-dCTP fluorescent dyes (GE Healthcare Life Sciences). Microarray slide preparation, probe-target hybridization, and washing steps were performed as described previously<sup>31</sup>. A total of 6 hybridization experiments were performed, including technical (i.e. dye-flip) replicates, in which the relative abundance of transcripts in variety T was compared with those of varieties L, 11 and 40, respectively (i.e. duplicate experiments for each of T vs L, T vs 11 and T vs 40). Fluorescence signatures were captured using a Scanarray 5000 scanner (PerkinElmer, Waltham, MA; <http://www.perkinelmer.com>) and analyzed using the TIGR TM4 suite of microarray tools<sup>34</sup>. Poor quality, low intensity or missing spots were flagged and excluded from further analysis. Florescence signals for each experiment were subjected to LOWESS normalization, followed by manual analysis. Transcripts that were potentially less or more abundant in T compared with the other varieties were identified using a signal intensity ratio cutoff of 1.8. Based on this criterion, eight genes were putatively underexpressed in T compared with at least two other varieties. Only one of these eight genes, represented on the microarray as the EST sequence 06\_B04 (GenBank accession FE964517) originating from the cell culture cDNA library was putatively underepxressed in T compared with all three morphine-producing varieties.

### **Expression vector construction**

The EST sequence 06\_B04 (GenBank accession FE964517) identified using microarray analysis was used to query an EST database containing 10,148 sequences from elicitor-treated cell cultures<sup>31</sup> and 7,949 sequences from stems of opium poppy using the tBLASTn algorithm. Although the 06\_B04 cDNA was incomplete, a full-length cDNA (named DIOX1) was identified in the cell culture EST database.

Two additional, full-length cDNAs with substantial nucleotide identity to DIOX1 were identified in the cell culture (DIOX2, 86%) and stem (DIOX3, 67%) cDNA libraries. Open reading frames (ORFs) encoding DIOX1, DIOX2 and DIOX3 were amplified from cDNA templates with *taq* polymerase (Invitrogen, Carlsbad, CA; <http://www.invitrogen.com>), using sense and antisense primers with flanking *Bam*HI and *Pst*I restriction sites, respectively (Supplementary Table 2). PCR products were individually ligated to pGEM-T (Promega, Madison, WI; <http://www.promega.com>), digested with *Bam*HI and *Pst*I, and ligated to pQE30 (Qiagen, Valencia, CA; <http://www.qiagen.com>) pre-cut with *Bam*HI and *Pst*I. DNA sequencing of cloned amplicons was performed following ligation into pGEM-T and pQE30 vectors (UCDNA Services, University of Calgary). Plasmid propagation was performed in the *Escherichia coli* strain XL1-Blue, and expression constructs were transformed into *E. coli* strain SG13009 to generate recombinant enzymes.

## Protein expression and purification

Production of DIOX1, DIOX2 and DIOX3 proteins in *E. coli* cultures was induced with 0.3 mM isopropyl  $\beta$ -D-thiogalactopyranoside (IPTG) followed by incubation at either 20°C for 4 hours (DIOX1 and DIOX2) or 4°C for 24 hours (DIOX3). Cells were harvested and bacterial pellets were resuspended in Buffer A (100 mM Tris-HCl pH 7.4, 10% (v/v) glycerol and 14 mM 2-mercaptoethanol). Lysis was achieved using a French Press at 0.1 GPa (15,000 psi) and lysates were cleared by centrifugation at 10,000*g* for 10 min. Cleared lysates were loaded onto Talon cobalt affinity columns (Clontech, Mountain View, CA; <http://www.clontech.com>) and purified, His-tagged proteins were eluted according to the manufacturer's instructions. The columns with protein bound were washed with Buffer A, and recombinant proteins were eluted using Buffer A containing 100 mM imidazole. Desalting was performed using PD10 columns (GE Healthcare Life Sciences) and protein concentrations were determined using the Bio-Rad Protein Assay (Bio-Rad, Hercules, CA; <http://www.bio-rad.com>). The purity of recombinant proteins was determined using SDS-PAGE<sup>35</sup>.

## Enzyme assays

The direct enzyme assay for 2-oxoglutarate-dependent dioxygenase activity was performed using a reaction mixture of 100 mM Tris-HCl (pH 7.4), 10% (v/v) glycerol, 14 mM 2-mercaptoethanol, 1 mM alkaloid, 10 mM 2-oxoglutarate, 10 mM sodium ascorbate, 0.5 mM FeSO<sub>4</sub>, and up to 100  $\mu$ g of purified recombinant enzyme. Assays were carried out at 30°C for 1 or 4 hours, stopped by immersing the reaction tube in boiling water for 5 min, and subjected to LC-MS/MS analysis. 2-Oxoglutarate-dependent dioxygenase activity was also assayed using an indirect method based on the *O*-demethylation-coupled decarboxylation of [1-<sup>14</sup>C]2-oxoglutarate<sup>14</sup>. Briefly, the standard assay contained 10  $\mu$ M of a 10% mole/mole (n/n) solution of [1-<sup>14</sup>C]2-oxoglutarate (specific activity 55 mCi/mmol) diluted with 90% n/n unlabeled 2-oxoglutarate, 10  $\mu$ M unlabelled alkaloid substrate, 10

mM sodium ascorbate, 0.5 mM iron sulfate, and 5  $\mu$ g purified enzyme in a 500  $\mu$ l buffered (100 mM Tris-HCl, 10% [v/v] glycerol, 14 mM 2-mercaptoethanol, pH 7.4) reaction. Assays were initiated by the addition of enzyme, incubated for 45 min at 30°C, and stopped by removing the  $^{14}\text{CO}_2$ -trapping glass fiber filters (Whatman grade GF/D, pretreated with NCS-II tissue solubilizer, Amersham Biosciences) from the reaction vial. For enzyme kinetic analyses, 10  $\mu$ M of a 1% (n/n) solution of [ $1\text{-}^{14}\text{C}$ ]2-oxoglutarate (specific activity 55 mCi/mmol) diluted with 99% (n/n) unlabeled 2-oxoglutarate was used. Results from assays lacking an alkaloid substrate were subtracted from corresponding assays containing alkaloid substrates to account for the uncoupled consumption of 2-oxoglutarate. Kinetic data for T6ODM were obtained by varying the thebaine or oripavine concentrations in the reaction between 1 and 500  $\mu$ M at a constant 2-oxoglutarate concentration of 500  $\mu$ M. Conversely, the 2-oxoglutarate concentration was varied between 1 and 500  $\mu$ M at a constant thebaine concentration of 30  $\mu$ M, which produced the maximum reaction velocity (Supplementary Fig. 10). Kinetic data for CODM were obtained by varying the of 500  $\mu$ M, and varying the 2-oxoglutarate concentration between 1 and 500  $\mu$ M at a constant codeine concentration of 50  $\mu$ M. Saturation curves and kinetic constants were calculated based on Michaelis-Menten kinetics using FigP v. 2.98 (BioSoft, Cambridge, UK; <http://www.biosoft.com>). The release of formaldehyde upon alkaloid *O*-demethylation was monitored using using a fluorescence-based modification of the Nash assay<sup>21</sup>. Nash reagent was prepared by adding 0.3 ml of glacial acetic acid and 0.2 ml acetyl acetone to 100 ml of 2 M ammonium acetate. Enzyme assays were performed as described above, except that unlabelled 2-oxoglutarate was used and the reactions were quenched by the addition of 2 volumes of Nash reagent, followed by a 10 min incubation period at 60°C to convert formaldehyde to diacetyldihydrolutidine (DDL). The fluorescence of DDL was recorded using a Cary Eclipse fluorescence spectrophotometer (Varian; [www.varianinc.com](http://www.varianinc.com)) at  $\lambda_{\text{ex}}$  = 412 nm and  $\lambda_{\text{em}}$  = 505 nm. The acylcyclohexanediones, prohexadione calcium or trinexapac-ethyl, were tested as possible enzyme inhibitors at concentrations up to 500  $\mu$ M using 100  $\mu$ M 2-oxoglutarate in a standard assay.

### Liquid chromatography-tandem mass spectrometry

Enzyme assays were diluted 1:10 with 0.1% (v/v) formic acid (morphinan alkaloids) or 0.2% acetic acid (protoberberine alkaloids) and analyzed using a 6410 Triple Quadrupole LC-MS/MS system (Agilent Technologies; Santa Clara, CA; <http://www.agilent.com>). Liquid chromatography was performed using a Zorbax Eclipse Plus C<sub>18</sub> column (2.1 x 50 mm, 1.8  $\mu$ m particle size; Agilent Technologies) at a flow rate of 0.4 ml/min. For morphinan alkaloids, the column was equilibrated in solvent A and alkaloids were eluted using a linear gradient to 100% solvent B over 4 min [solvent A: 20% (v/v) acetonitrile/0.1% (v/v) formic acid/79.9% (v/v) water; solvent B: 99.9% (v/v) acetonitrile/0.1% (v/v) formic acid]. For protoberberine alkaloids, the column was equilibrated in solvent C and alkaloids were eluted under the following conditions: 0-1 min 0% solvent D, 1-10 min to



35% solvent D, 10-11 min to 100% solvent D [solvent C: 2% (v/v) acetonitrile/0.2% (v/v) acetic acid/97.8% (v/v) water; solvent D: 98% (v/v) acetonitrile/0.2% (v/v) acetic acid/2% (v/v) water]. Injection into the mass analyzer was performed using an electrospray ionization (ESI) probe inlet. Ions were generated and focused using an ESI voltage of 4000 kV, 9 l/min gas flow, 40 psi nebulizing pressure, and gas temperature of 330°C. MS data acquisition was carried out in positive ion mode over 50-400 *m/z*. The collision-induced dissociation (CID) mass spectra were recorded using collision energies of -15.0 eV (thebaine and oripavine), -25.0 (codeinone, morphinone, scoulerine and 3-*O*-demethylscoulerine), -32.0 eV (morphine) and -30.0 eV (codeine). Argon collision gas was set at a pressure of  $1.8 \times 10^{-3}$  torr. Alkaloids were identified based on either previously published ESI mass spectra<sup>36,37</sup> or by comparison with ESI mass spectra of authentic standards.

## Virus-induced gene silencing

**Construction of vectors** – Unique 3'-UTR sequences were used for the construction of virus-induced gene silencing (VIGS) vectors to specifically silence genes encoding DIOX1, DIOX2 and DIOX3, and to avoid the suppression of highly homologous genes: DIOX-b (*DIOX1*-specific; 221 bp), DIOX-c (*DIOX2*-specific; 152 bp) and DIOX-d (*DIOX3*-specific; 292 bp)<sup>38</sup>. In addition, a construct was assembled for the purpose of simultaneously silencing *DIOX1*, *DIOX2* and *DIOX3*. The design of this non-specific construct (DIOX-a; 342 bp) was based on a highly conserved ORF sequence in all three genes. Full-length cDNA clones were used as templates to amplify fragments shown in Supplementary Fig. 12. Forward and reverse PCR primers were designed with flanking *Bam*HI and *Xho*I restriction endonuclease sites, respectively (Supplementary Table 2). Amplicons were generated using *Taq* DNA polymerase (Invitrogen), ligated to pGEM-T (Promega), digested with *Bam*HI and *Xho*I, and isolated inserts ligated to pTRV2<sup>39</sup> pre-cut with *Bam*HI and *Xho*I. DNA sequencing of cloned products was performed after ligation into both vectors. Plasmid propagation was achieved in the *E. coli* strain XL1-Blue, and the pTRV2 constructs (i.e. DIOX-a, DIOX-b, DIOX-c, DIOX-d and the empty vector) and pTRV1<sup>39</sup> were independently mobilized in *Agrobacterium tumefaciens* strain GV3101.

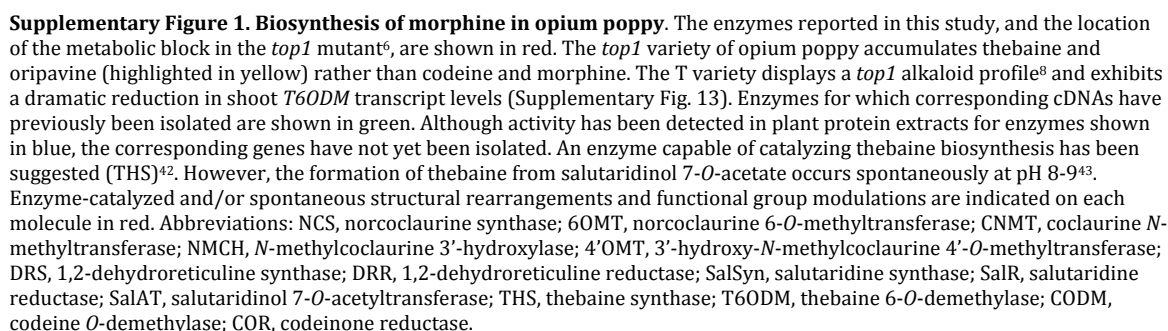
**Infiltration of plants** – Bacteria were prepared for infiltration using a previously reported protocol<sup>40</sup>. Independent overnight liquid cultures of *A. tumefaciens* containing each construct were used to inoculate 500 ml of Luria-Bertani (LB) medium containing 10 mM MES, 20  $\mu$ M acetosyringone and 50  $\mu$ g/ml kanamycin. Cultures were maintained at 28°C for 24 hours, harvested by centrifugation at 3000*g* for 20 min, and resuspended in infiltration solution (10 mM MES, 200  $\mu$ M acetosyringone, 10 mM MgCl<sub>2</sub>) to an OD<sub>600</sub> of 2.5. *Agrobacterium tumefaciens* harboring DIOX-a, DIOX-b, DIOX-c, DIOX-d and the pTRV2 empty vector were each mixed 1:1 (v/v) with *A. tumefaciens* containing pTRV1, and incubated for one hour at 20°C prior to infiltration. Opium poppy plants used for VIGS analysis were 2-3 weeks old with emerging first leaves. Infiltration of the *A. tumefaciens* inoculum to the emerging leaves was performed using a 1-cc syringe. Plants inoculated with pTRV1 and pTRV2, the latter

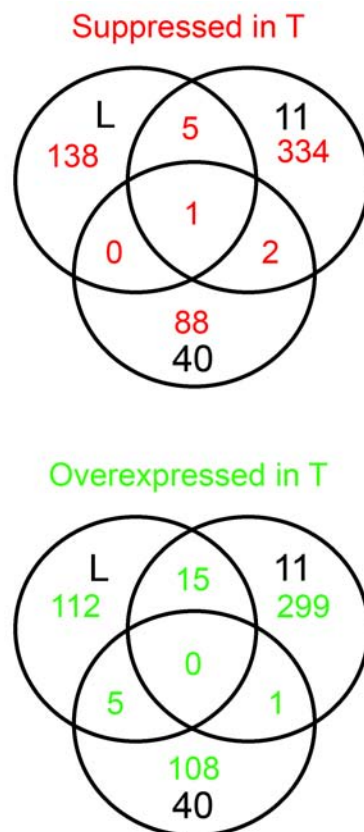
containing a fragment of the opium poppy gene encoding phytoene desaturase (PapsPDS)<sup>40</sup>, displayed photobleaching and were used as a visual marker of VIGS efficiency, which was typically in the range of 20-25%.

*Metabolite profiling* – Infiltrated opium poppy plants were analyzed at maturity (i.e. the emergence of flower buds). Stems were cut immediately below the flower bud and 10 µl of exuding latex was collected. At the same time, three 1-cm segments of stem tissue directly below the flower bud were excised and flash frozen in liquid nitrogen for RT-qPCR analysis. Initial phenotypic screening was performed by thin layer chromatography (TLC). Latex samples were suspended in 30 µl methanol and 10 µl was spotted on TLC Silica gel 60 F<sub>254</sub> plates (Merck). Separation was achieved using a previously described solvent system<sup>6</sup> and alkaloids were visualized by shadowing under 254 nm UV illumination. Major alkaloids were identified based on the comparison of R<sub>f</sub> values with those of authentic standards. TLC results were confirmed using high performance liquid chromatography (HPLC) as described previously<sup>8</sup>. Fifteen microliters of methanol-latex suspension was diluted with 235 µl of methanol, vortexed and centrifuged for 10 min at 10,000g to remove insoluble debris and 100 µl of the supernatant was analyzed by HPLC.

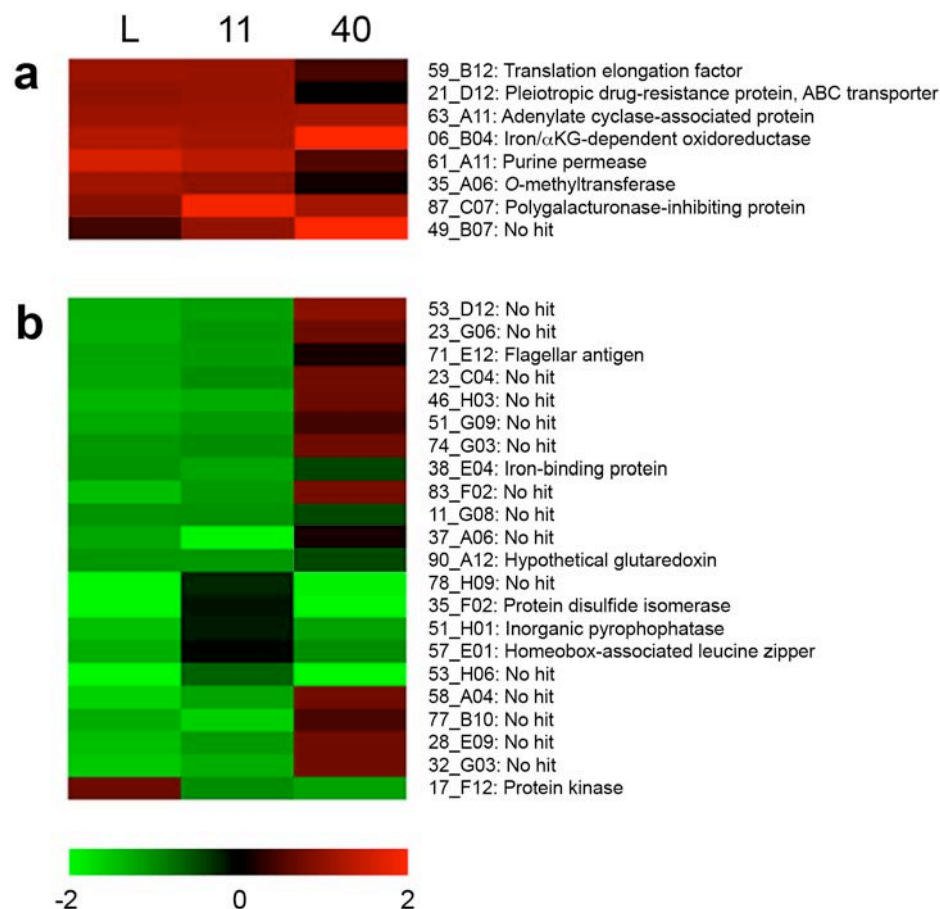
## Gene expression analysis

Total RNA was isolated with TRIzol (Invitrogen) according to the manufacturer's instructions. Reverse transcription was performed at 42°C for 60 min using 2.5 mM anchored oligo(dT) primer (dT20VN), 0.5 mM dNTP, 10 to 40 ng/µl RNA, and 5 microunits/ul reverse transcriptase (Fermentas, Burlington, Canada; <http://www.fermentas.com>) following denaturing of the RNA-primer mix at 70°C for 5 min. Real-time quantitative PCR using SYBR Green detection was performed using a 7300 Real-Time PCR system (Applied Biosystems). Each 10-µL PCR included 1 µL of cDNA (taken directly from the RT reaction in the case of stem, or diluted 50% [v/v] with water for bud, leaf and root), 300 nM forward and reverse primers, and 1x Power SYBR Green PCR Master Mix (Applied Biosystems). Primer sequences are listed in Supplementary Table 2. Reactions were subjected to 40 cycles of template denaturation, primer annealing and primer extension. To evaluate qPCR specificity, the amplicons of all primer pairs were subjected to melt-curve analysis using the dissociation method suggested by the instrument manufacturer (Applied Biosystems). Gene expression data for VIGS analysis were determined based on 27 independent values per plant line (i.e. 3 technical replicates performed on each of 3 stem segments taken from each of 3 individual plants). Organ-specific gene expression data (Supplementary Fig. 13) were based on nine independent values per plant line (i.e. 3 technical replicates on each of 3 individual plants). The 2<sup>-ΔΔCt</sup> method was used for the analysis of relative gene expression<sup>41</sup> as described previously<sup>8</sup>. The gene encoding elongation factor 1a (elf1a) was used as the internal control and the plant line showing the highest expression level served as the calibrator for each target gene.



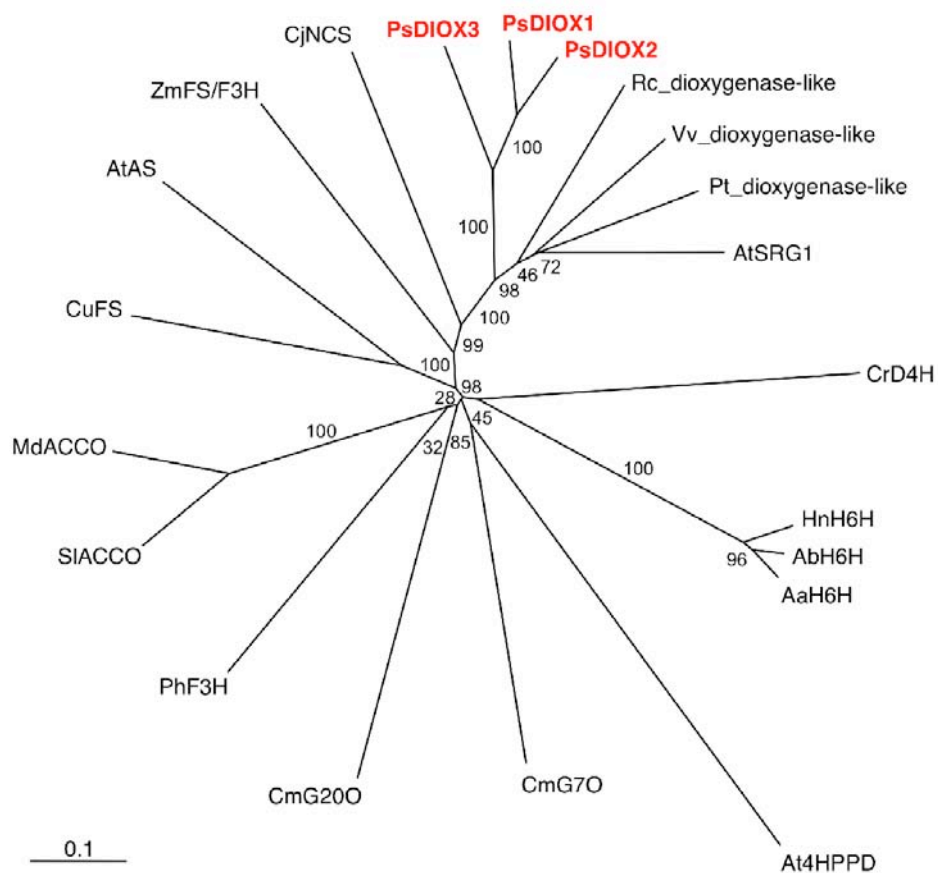


**Supplementary Figure 2. Venn diagrams summarizing the results of microarray hybridization experiments that compared the abundance of transcripts in the stems of opium poppy variety T with varieties L, 11 and 40.** The numbers of genetic elements on the microarray that showed decreased hybridization of RNA from variety T compared with varieties L, 11 and/or 40 are indicated in the upper panel (red). Conversely, the numbers of genetic elements that showed increased hybridization of RNA from variety T compared with varieties L, 11 and/or 40 are indicated in the lower panel (green). Decreased or increased hybridization was indicative of lower or higher transcript abundance, respectively, and thus revealed a relative suppression in the expression of specific genes. Genes were considered differentially expressed based on a signal intensity ratio cutoff of 1.8. Microarray hybridization experiments involving pair-wise comparisons of varieties T vs L, T vs 11, and T vs 40 revealed eight genes putatively suppressed in T compared with at least two other varieties, but only a single gene suppressed in T compared with all three varieties (upper panel).



**Supplementary Figure 3. Heat maps illustrating the relative abundance of transcripts in the stems of opium poppy variety T with varieties L, 11 and 40.** Results are shown only for genes exhibiting low (a) or high (b) expression in T compared with at least two other varieties, based on a ratio cutoff of 1.8. Corresponding functional annotations and microarray coordinates are shown to the right of each diagram. Average signal intensity ratios from 6 independent microarray hybridization experiments were  $\log_2$  normalized and plotted based on the indicated color scheme. Positive values (red color) indicate relatively lower transcript levels in variety T, whereas negative values (green color) indicate relatively higher transcript levels in variety T compared with varieties L, 11 and 40. Images were generated using MultiExperiment Viewer (TIGR TM4 Microarray Software Suite)<sup>34</sup>. Note that 06\_B04 in (a) corresponds to DIOX1, which was renamed T6ODM after functional characterization.

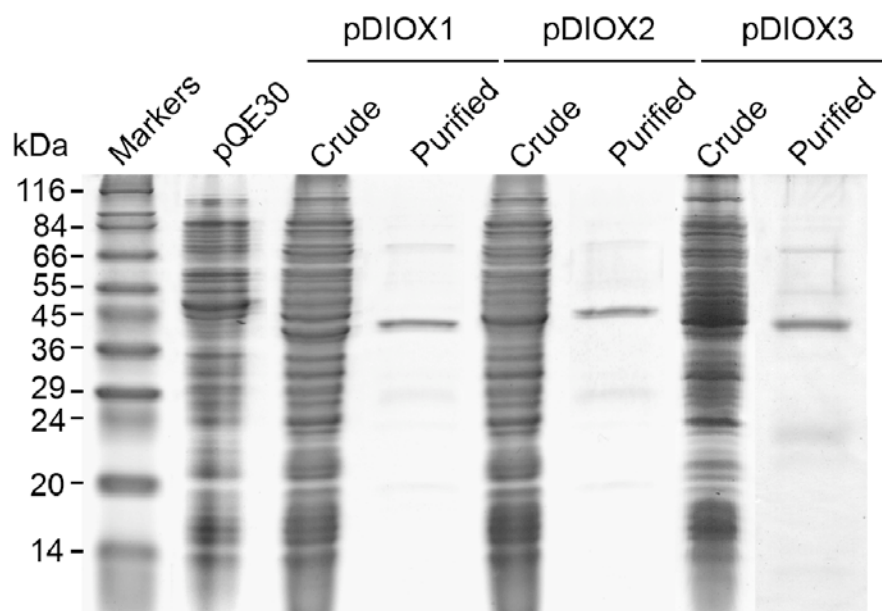




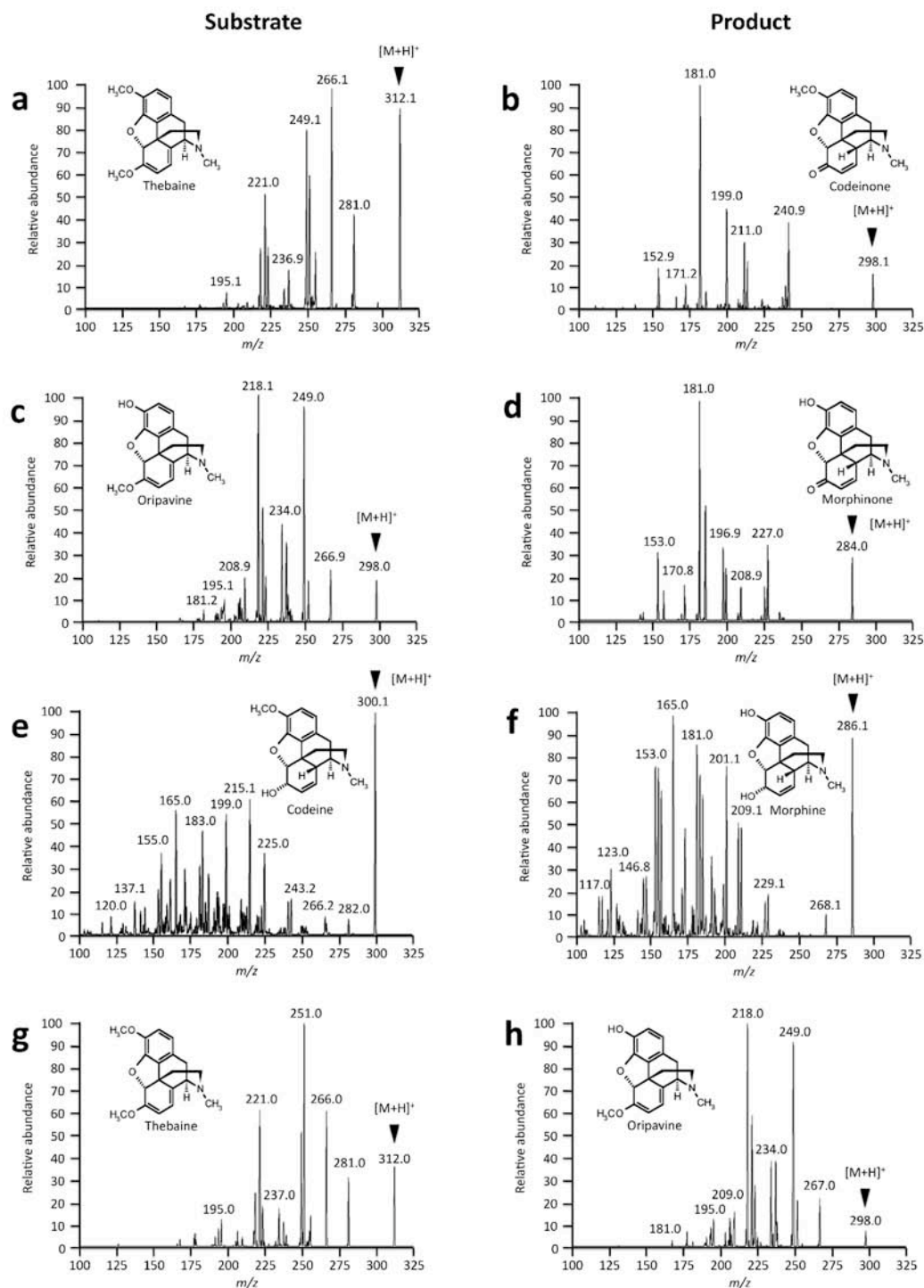
**Supplementary Figure 4. Unrooted neighbor-joining phylogenetic tree for selected plant 2-oxoglutarate (2OG)/Fe(II)-dependent dioxygenases.** Bootstrap frequencies for each clade are percentages of 1,000 iterations. Bootstrapping provides several alternative versions of the branch points that separate each of the different clades. The bootstrap value indicates the frequency of a branch occurring at the indicated position in alternative phylogenetic analyses. Abbreviations and GenBank accession numbers are listed in the phylogenetic analysis section of the Methods. Note that DIOX1 and DIOX3 were renamed thebaine 6-*O*-demethylase (T6ODM) and codeine *O*-demethylase (CODM), respectively, after functional characterization.

		.10	.20	.30	.40	.50	.60																																																					
PsDIOX1	..	..	..	..	MEKAKLMKLGNGMEIP	SVQELAKL	24																																																					
PsDIOX2	..	..	..	..	METAKLMKLGNGMSIP	SVQELAKL	24																																																					
PsDIOX3	..	..	..	..	METPIILKLGNGLSIP	SVQELAKL	24																																																					
AtSRG1	..	..	..	..	MEAKGAAQWSS..IL	VPVQEMVKE	23																																																					
CjNCS	..	..	..	..	MSKNLTGVGGSLPVEN	VQVLAGK	23																																																					
HnH6H	..	..	..	..	..	MATFVS	7																																																					
CrD4H	MPKSWPIV	ISSHSFCFLPNSE	QERKMKDLNFHAATLS	SEESLRE	LKAFDET	KAGVKGIVD	60																																																					
		.70	.80	.90	100	110	120																																																					
PsDIOX1	..	TLAEIP	SRVVCANENLL	PMGASVINDHET	IPVIDIENLL	SPEPIIGKLELDRL	HFAK	83																																																				
PsDIOX2	..	TLAEIP	SRVICTVENL	QLPVGASVIDD	HETVPVIDIENLL	SSEPVT	EKLELDRLHSAK	83																																																				
PsDIOX3	..	TLAEIP	SRVCTGESPL	NNIGASVTD	ETVPVIDLQNL	SPVPVVKLELDRL	HSAK	82																																																				
AtSRG1	K	ITTVPR	YVRSDQD..	KTEVDDDF	DKIEIP	IDMKRLCS	..TTMDSE	VEKLDFAK	79																																																			
CjNCS	..	EIKNLE	NRVVRPELE..	HDDVVPID	NSLEIP	VIDLSRLDQ	..YACDEL	AKFHSACK	77																																																			
HnH6H	W	STKS	VSESFIA	PLQKR..AEK	DVPVGN..DVP	IDLQHHHL	..LVQQIT	KACQ	56																																																			
CrD4H	TG	ITK	LRIFID	QPKNLD	RISVCRGKS	D..IKLP	VINLNGLS	NS..EIRREI	VEKIG	118																																																		
		130	140	150	160	170	180																																																					
PsDIOX1	EW	GFQV	VNHGVD	ASLVDS	VKSEIQ	GFNLSMDEK	TYEQE	....	DGDVE	GFGQGF	137																																																	
PsDIOX2	EW	GFQV	VNHGVD	TSLVD	NVKS	DIQGF	NLSMNEK	IYKQ	....	DGDVE	GFGQAF	137																																																
PsDIOX3	EW	GFQV	VNHGVD	ALLMD	NIKSEI	KGFNLP	MEKIKYQ	....	DGDVE	GFGQPYI	136																																																	
AtSRG1	EW	GFQV	VNHG	ISSFL	DKV	KSEIQ	GFNLP	MEKIKFWOR	....	PDEI	EFGQAF	133																																																
CjNCS	D	MGFF	QLIN	HGVREE	VIKMK	VDTE	DFRL	PFKEKNATROL	....	PNGME	GYQAF	131																																																
HnH6H	D	FG	QV	IN	HGF	PEEL	MLET	MEVCKE	FFAL	PAEKEK	FKPKGAAK	FELPLE	QAKLYE	116																																														
CrD4H	KY	GFQV	VNHG	IPQD	VMD	KMVD	GV	VRKFE	QDDQ	IKRQYSR	....	DRFN	KNF	LYSS	NYVL	174																																												
		190	200	210	220	230	240																																																					
PsDIOX1	SE	...	DQ	LDWAD	IFMM	FTLPL	HLRK	PHLF	SKLP	VP	PRE	TIES	SY	SEM	KKLS	SMV	LF	NKM	193																																									
PsDIOX2	SE	...	DQ	LDWAD	IFM	ITLPL	HLRK	PHLF	SKLP	LP	PRE	TIES	SY	SEM	KKLS	SMV	LF	NKM	193																																									
PsDIOX3	SE	...	DQ	LDWTE	VF	SMLS	PLHL	RKPH	LFPE	LP	PRE	TIES	SY	L	SKM	KKLS	STV	V	FEM	192																																								
AtSRG1	SE	...	DQ	KLDWAD	LF	FHTV	QV	ELR	KPH	LF	PKLP	PR	DTL	EM	YS	SE	VQ	SA	KIL	IAKM	189																																							
CjNCS	SE	...	EQ	KLDWAD	MH	FLIT	KPVQ	ERN	MR	F	WPT	SPT	S	PRE	T	ME	KYS	ME	LQ	VAM	CLTGM	187																																						
HnH6H	GE	Q	LSNE	E	FLY	WKD	TLA	H	GCH	PLD	QDL	V	NSW	PEK	PA	KY	RE	V	A	KYS	VE	VRK	L	MR	MLD	YI	176																																	
CrD4H	IP	...	GI	ACN	WRD	T	ME	C	I	M	S	N	Q	P	D	...	Q	E	F	P	D	V	C	R	D	I	L	M	K	Y	S	N	Y	V	R	N	L	G	L	I	L	F	E	L	226															
		250	260	270	280	290	300																																																					
PsDIOX1	E	KALQ	VQAA	EIK	MSE	V	FID	G	TQ	AM	R	N	Y	P	P	C	P	Q	P	N	L	A	I	G	L	T	S	H	S	D	F	G	G	L	T	I	L	L	Q	N	E	V	253																	
PsDIOX2	E	KALQ	VQAA	EIK	E	IS	V	F	K	D	M	T	Q	V	M	R	N	Y	P	P	C	P	Q	P	E	L	A	I	G	L	T	S	H	S	D	F	G	G	L	T	I	L	L	Q	N	E	V	253												
PsDIOX3	E	KSLQ	...	VEI	K	G	M	T	D	L	F	E	D	G	L	Q	T	M	R	N	Y	P	P	C	P	R	P	E	L	V	L	G	L	T	S	H	S	D	F	S	G	L	T	I	L	L	Q	N	E	V	250									
AtSRG1	A	R	A	L	E	I	K	P	E	E	L	K	L	F	D	...	V	D	S	V	S	M	R	N	Y	P	P	C	P	Q	P	D	Q	V	I	G	L	T	S	H	S	D	S	V	G	L	T	I	L	L	Q	N	E	V	248					
CjNCS	A	N	L	G	...	E	S	E	I	L	T	K	...	L	R	T	V	F	N	R	E	D	E	L	L	S	M	S	S	C	G	E	G	L	G	L	S	P	H	S	D	A	T	G	L	T	I	L	L	Q	N	E	V	243						
HnH6H	C	E	G	L	G	...	K	L	G	F	D	N	E	L	S	Q	I	Q	M	L	T	N	Y	P	P	C	P	D	P	S	T	L	G	S	G	H	Y	D	G	N	L	I	T	L	L	Q	D	L	P	G	232									
CrD4H	S	E	A	L	G	...	K	P	N	H	L	E	M	D	C	A	E	G	L	I	L	G	H	Y	P	A	C	P	Q	P	E	L	T	F	G	T	S	K	H	S	D	S	G	F	L	T	I	L	M	Q	D	...	Q	I	282					
		310	320	330	340	350	360																																																					
PsDIOX1	E	G	L	Q	I	K	R	E	G	T	W	I	S	V	K	P	L	P	N	A	F	V	V	N	V	G	D	I	L	E	I	M	T	N	G	I	T	S	V	D	H	R	A	V	V	N	S	T	N	E	R	L	S	I	A	T	F	H	D	313
PsDIOX2	E	G	L	Q	I	K	R	E	G	R	W	I	S	V	K	P	L	P	N	A	F	V	V	N	V	G	D	V	L	E	I	M	T	N	G	M	Y	S	V	D	H	R	A	V	V	N	S	T	N	E	R	L	S	I	A	T	F	H	D	313
PsDIOX3	E	G	L	Q	I	K	R	E	R	W	I	S	I	K	P	L	P	D	A	F	I	V	N	V	G	D	I	L	E	I	M	T	N	G	I	T	S	V	E	H	R	A	V	V	N	S	T	N	E	R	L	S	I	A	T	F	H	D	310	
AtSRG1	E	G	L	Q	I	K	D	G	K	W	P	V	K	P	L	N	A	F	I	V	N	I	G	D	V	L	E	I	T	N	G	T	S	I	E	H	R	G	V	V	N	S	E	K	E	R	L	S	I	A	T	F	H	N	308					
CjNCS	N	G	L	H	I	K	K	D	E	K	W	P	I	K	P	L	G	A	F	V	N	I	G	D	V	I	E	I	M	S	N	G	I	T	S	I	E	H	R	A	V	I	N	T	D	K	E	R	L	S	I	A	T	F	H	D	303			
HnH6H	L	Q	L	I	V	K	D	A	T	W	I	A	V	O	P	I	T	A	F	V	N	L	G	L	T	L	K	V	I	T	N	E	K	F	E	G	S	I	H	R	V	T	D	P	T	R	D	R	V	S	I	A	T	L	I	G	292			
CrD4H	G	G	L	Q	I	L	L	E	N	Q	W	I	D	V	P	F	I	P	G	A	L	V	I	N	I	A	D	L	L	Q	L	T	N	D	K	F	S	V	E	H	R	V	L	A	N	K	V	G	P	R	I	S	V	A	V	A	F	G	342	
		370	380	390	400	410	420																																																					
PsDIOX1	P	S	L	E	S	...	V	I	G	P	I	S	S	L	I	T	P	E	T	P	A	L	F	R	S	G	S	T	Y	G	D	L	V	E	E	C	K	T	R	K	L	D	G	K	S	F	L	D	S	M	R	I	..	364						
PsDIOX2	P	N	L	E	S	...	E	I	G	P	I	S	S	L	I	T	P	N	T	P	A	L	F	R	S	G	S	T	Y	G	E	L	V	E	E	F	H	S	R	K	L	D	G	K	S	F	L	D	S	M	R	M	..	364						
PsDIOX3	S	K	L	E	S	...	E	I	G	P	I	S	S	L	I	T	P	E	T	P	A	L	F	R	G	...	R	Y	E	D	I	L	K	E	N	L	S	R	K	L	D	G	K	S	F	L	D	Y	M	R	..	360								
AtSRG1	V	G	M	Y	K	...	E	V	G	P	A	K	S	L	V	E	R	O	K	V	A	R	E	K	R	L	...	T	M	K	E	Y	N	D	G	L	F	S	R	T	L	D	G	K	A	Y	L	D	A	L	R	..	358							
CjNCS	P	E	Y	G	T	...	K	I	G	P	L	P	D	L	V	K	...	E	N	G	V	K	Y	K	T	...	D	Y	E	D	Y	L	I	R	S	S	N	I	K	L	D	G	K	S	L	D	M	K	L	..	352									
HnH6H	P	D	Y	S	C	...	T	I	E	P	A	K	E	L	N	Q	D	N	P	L	Y	K	P	Y	...	S	Y	S	E	F	A	D	I	Y	L	S	D	K	S	D	Y	D	S	G	V	K	P	Y	K	I	N	V	344							
CrD4H	I	K	T	Q	T	Q	E	G	V	S	P	R	L	Y	G	P	I	K	E	L	I	S	E	N	P	I	Y	K	E	V	...	T	V	K	D	F	I	T	I	R	F	A	K	R	F	D	S	S	I	S	P	F	R	L	N	401				

**Supplementary Figure 5. Alignment of the deduced amino acid sequences of opium poppy DIOX1, DIOX2, and DIOX3 with other plant 2-oxoglutarate (2OG)/Fe(II)-dependent dioxygenases.** Sequences were aligned using ClustalX<sup>29</sup>. Shaded boxes indicate residues that are identical in at least 40% of the aligned proteins. Dots represent introduced gaps into sequences to maximize the alignment. Abbreviations: AtSRG1, *Arabidopsis thaliana* senescence-related gene 1; CjNCS, *Coptis japonica* norcoclaurine synthase; HnH6H, *Hyoscyamus niger* hyoscyamine 6 $\beta$ -hydroxylase, CrD4H, *Catharanthus roseus* desacetoxyvindoline 4-hydroxylase. Residues corresponding to a canonical HXDX<sub>n</sub>H catalytic triad (green triangles) required for coordinating Fe(II)<sup>19</sup> and a YX<sub>n</sub>RXS motif (red circles) implicated in 2OG binding<sup>10</sup> are indicated. Note that DIOX1 and DIOX3 were renamed thebaine 6-O-demethylase (T6ODM) and codeine O-demethylase (CODM), respectively, after functional characterization.

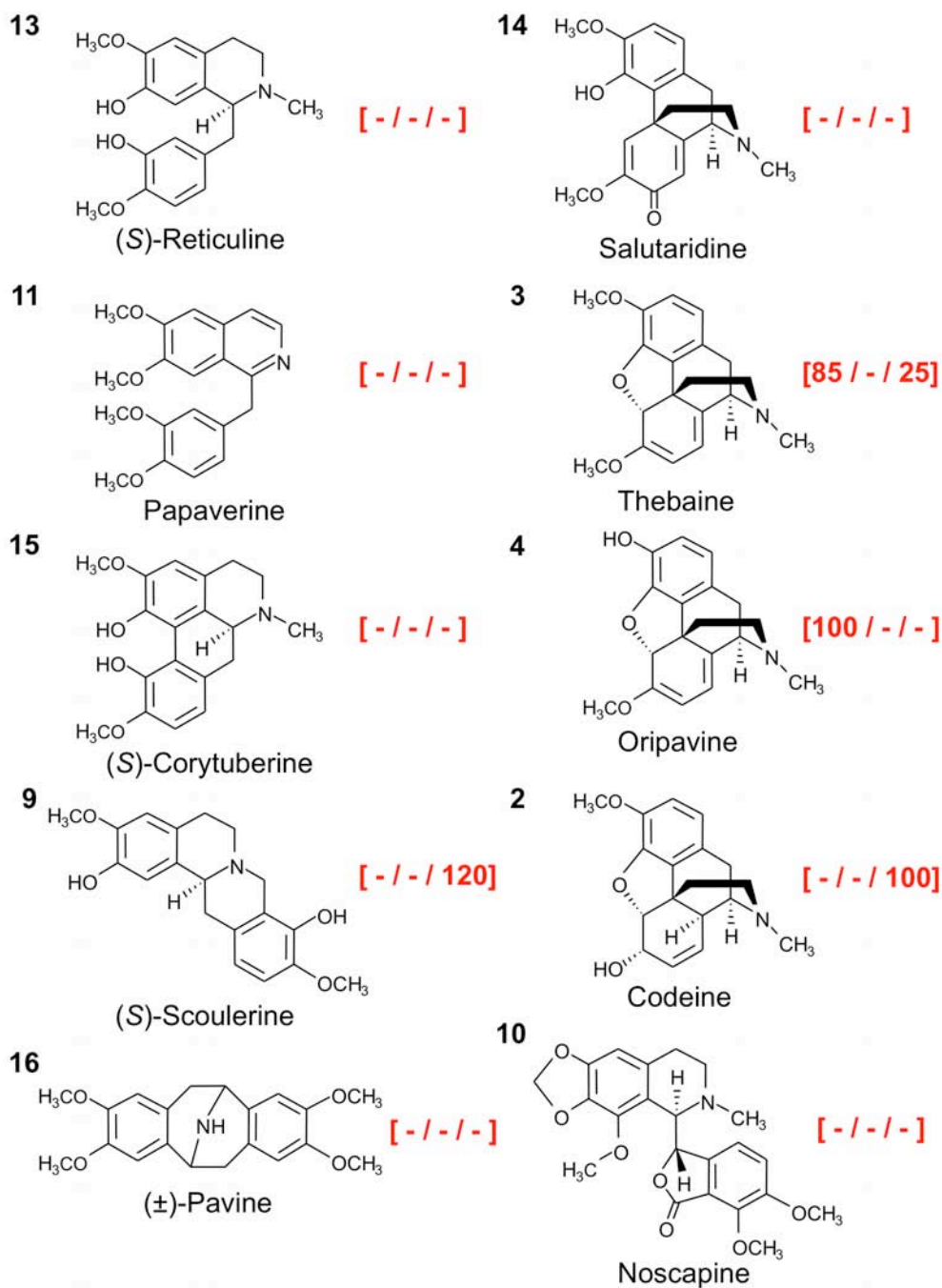


**Supplementary Figure 6. SDS-PAGE of recombinant proteins produced by pDIOX1 (thebaine 6-*O*-demethylase, T6ODM), pDIOX2, and pDIOX3 (codeine *O*-demethylase, CODM) in *Escherichia coli*.** The left lane contains molecular weight protein markers and corresponding sizes are indicated to the left of the panel. All other lanes feature total (crude) or purified protein from *E. coli* strain SG13009 cells induced with IPTG. Purification of polyhistadine-tagged recombinant proteins was achieved using a cobalt-affinity column. Bacteria harboring the empty pQE30 vector were included as a negative control. Visualization was achieved using Coomassie blue staining.



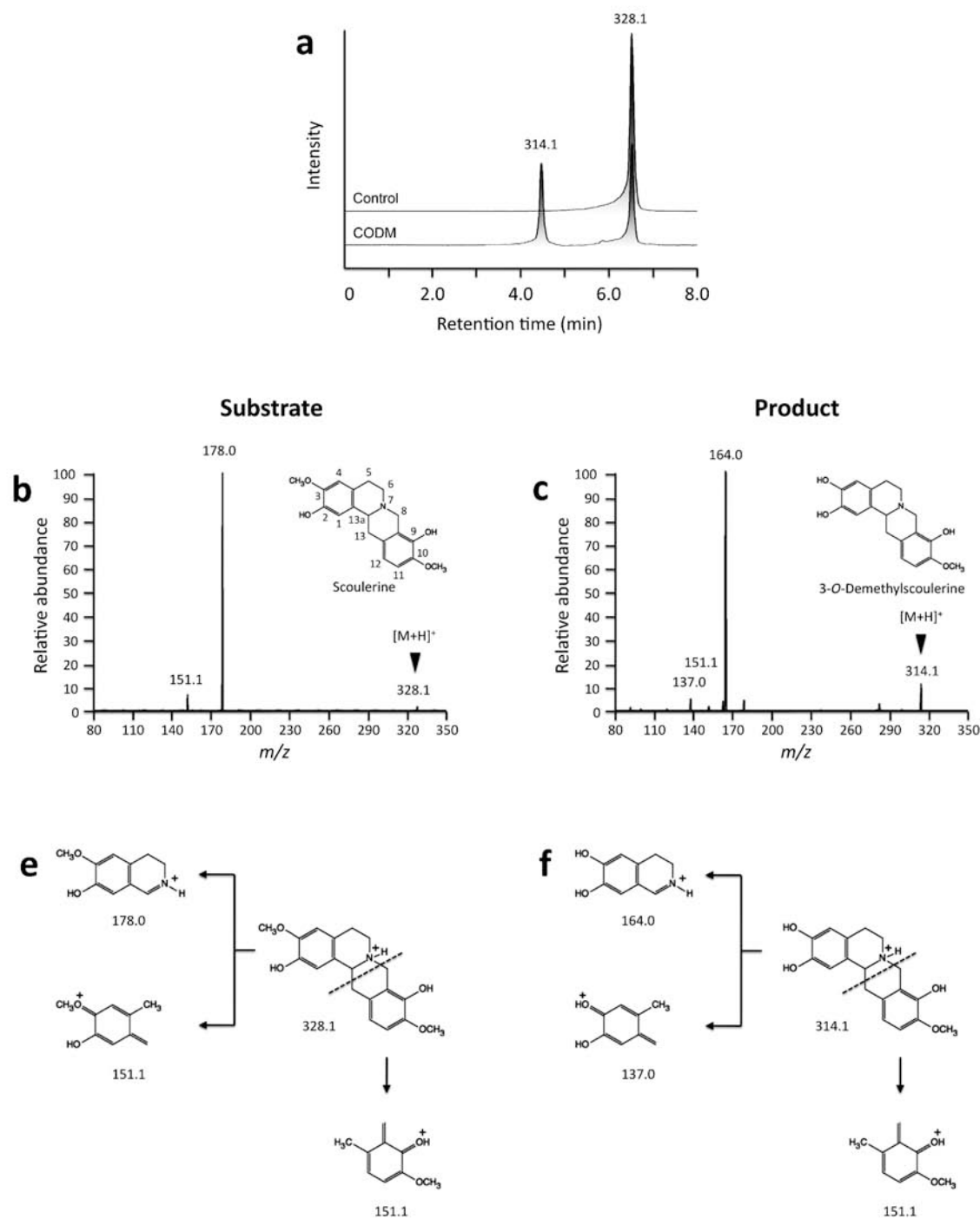
**Supplementary Figure 7. Collision-induced dissociation (CID) mass spectra for substrates (left panels) and products (right panels) of thebaine 6-*O*-demethylase (T6ODM, a-d) and codeine *O*-demethylase (CODM, e-h) enzyme assays.** Following liquid chromatography (LC), molecular parent ions (arrowheads) were generated and focused using electrospray ionization (ESI), and subjected to mass spectrometry. To unambiguously identify reaction components, daughter ions were generated using argon gas collision at the following energies: -15.0 eV (thebaine and oripavine), -25.0 (codeinone and morphinone), -32.0 eV (morphine) and -30.0 eV (codeine). The observed ESI mass spectra were in agreement with previously published ESI spectra<sup>36</sup> and with those acquired for authentic standards. Structures corresponding to the parent molecules are shown.



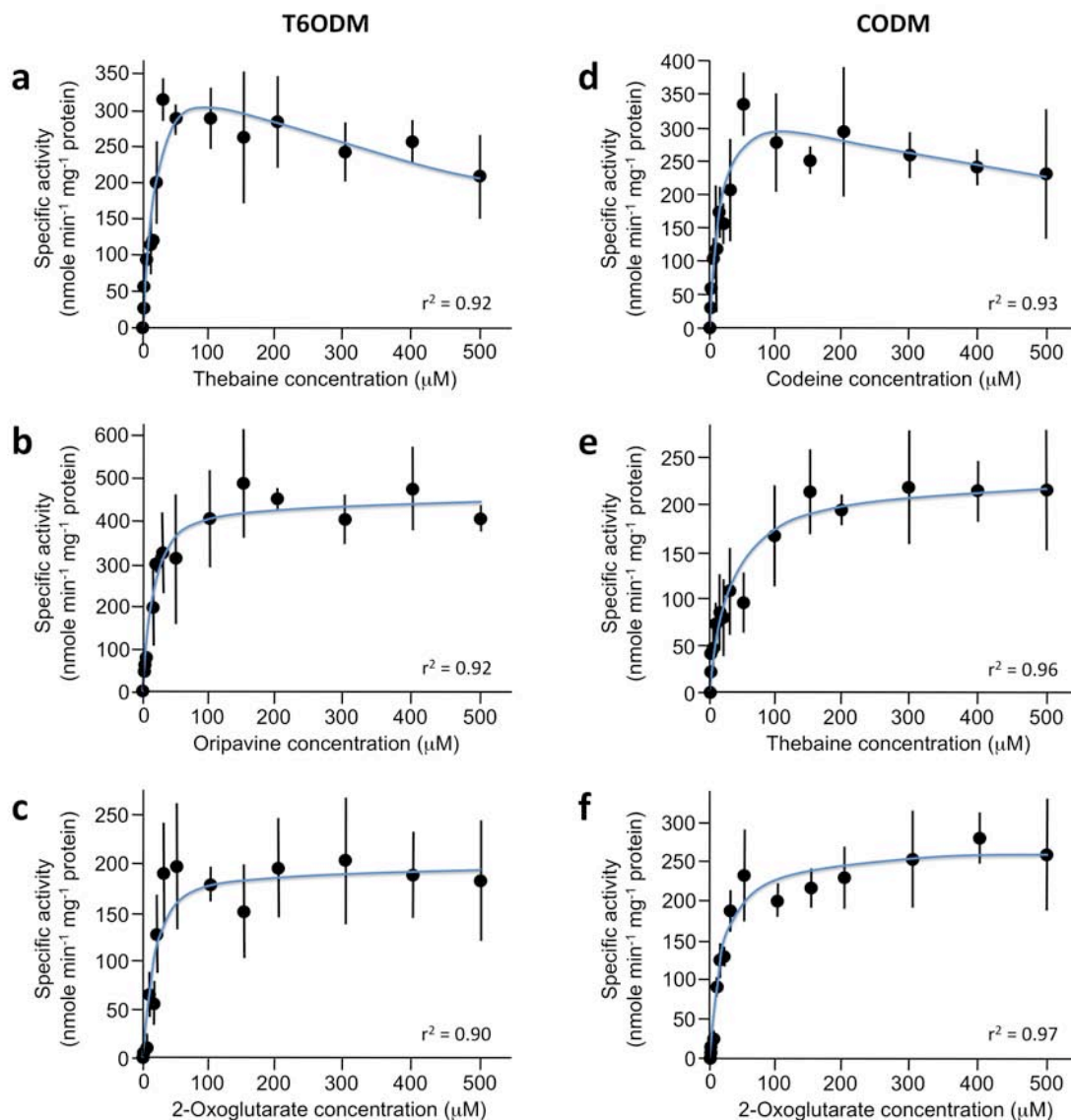


**Supplementary Figure 8. Substrate specificities of recombinant thebaine 6-*O*-demethylase (T6ODM), DIOX2 and codeine *O*-demethylase (CODM).** Enzyme assays were based on the decarboxylation of [1-<sup>14</sup>C]2-oxoglutarate coupled with the *O*-demethylation of a benzylisoquinoline alkaloid co-substrate. The incubation time (45 min), protein concentration (10 ng/μl) and other assay parameters were optimized prior to enzyme kinetic analyses. The structures of compounds tested as potential enzymatic substrates are shown adjacent to values indicating percent relative activities for T6ODM, DIOX2, and CODM, respectively. Hyphens indicate that enzyme activity was not detected.

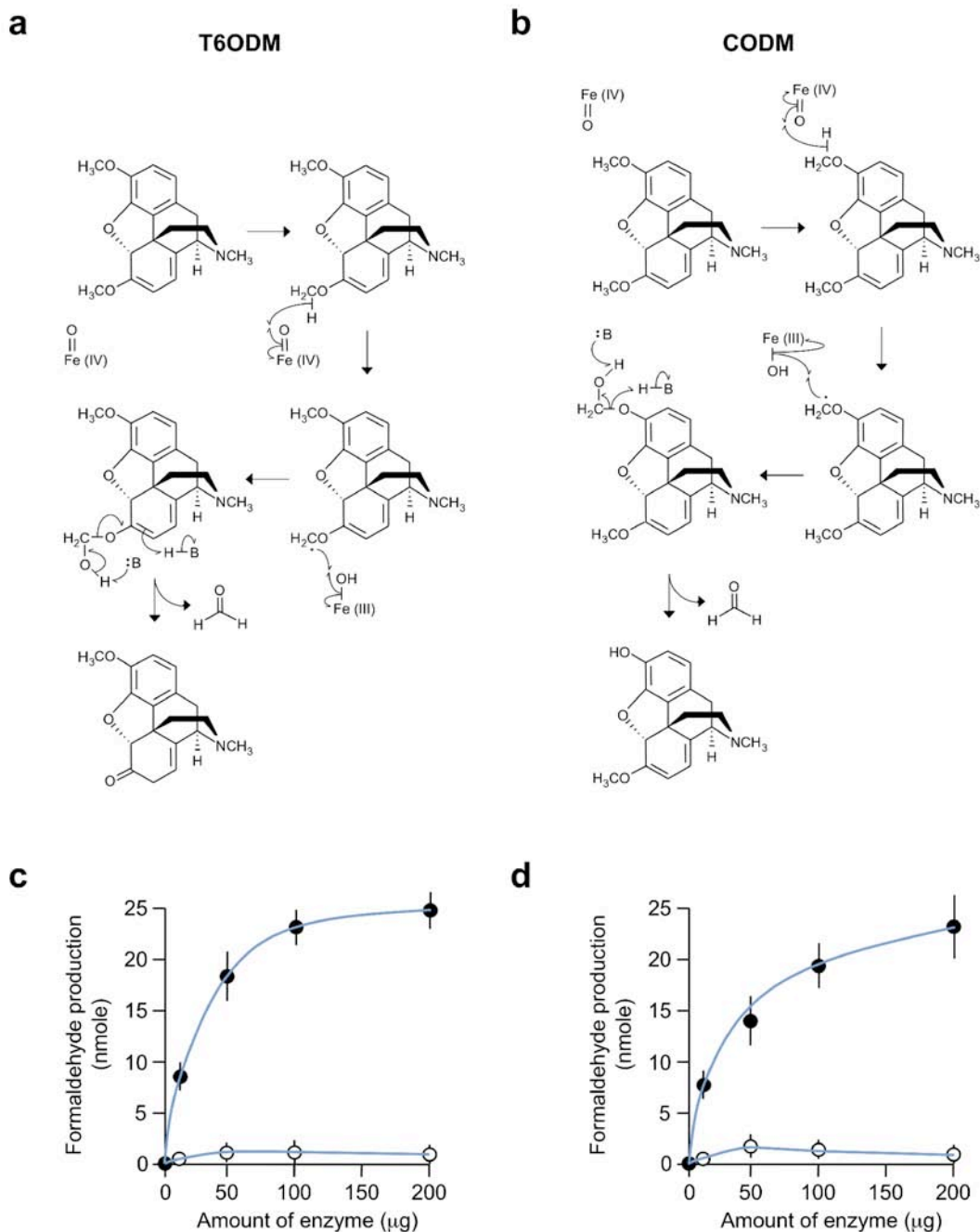




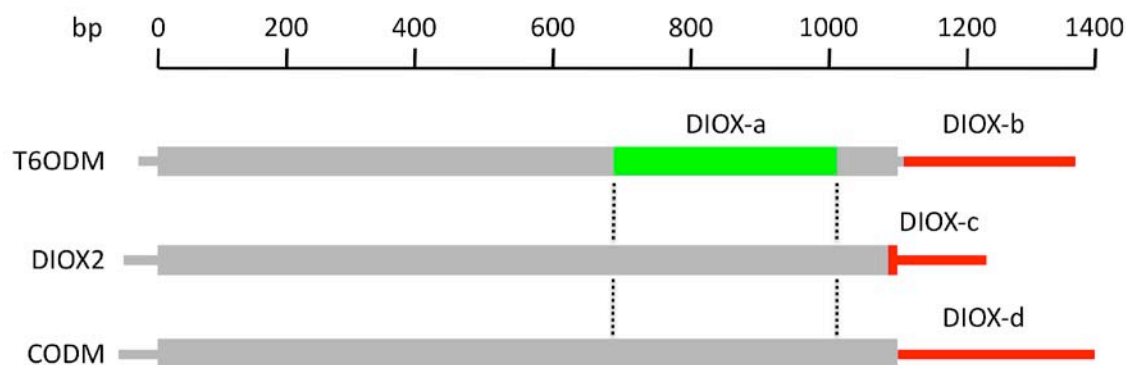
**Supplementary Figure 9. Extracted ion chromatograms (EICs) and collision-induced dissociation (CID) mass spectra showing the 3-*O*-demethylation of (*S*)-scoulerine by codiene *O*-demethylase (CODM). a**, The upper (control) EIC corresponds to an assay performed with boiled enzyme, whereas the lower (CODM) EIC shows an assay performed with native enzyme. Incubation of native CODM with (*S*)-scoulerine ( $m/z$  328.1) as the substrate yielded a reaction product of  $m/z$  314.1, consistent with the loss of a methyl group. CID analysis at a collision energy of -25.0 eV supported *O*-demethylation of (*S*)-scoulerine at position 3 (**b**) yielding 3-*O*-demethylscoulerine (**c**). Proposed mass spectral fragmentation of (*S*)-scoulerine (**e**) and 3-*O*-demethylscoulerine (**f**) under electrospray CID conditions<sup>37</sup>.



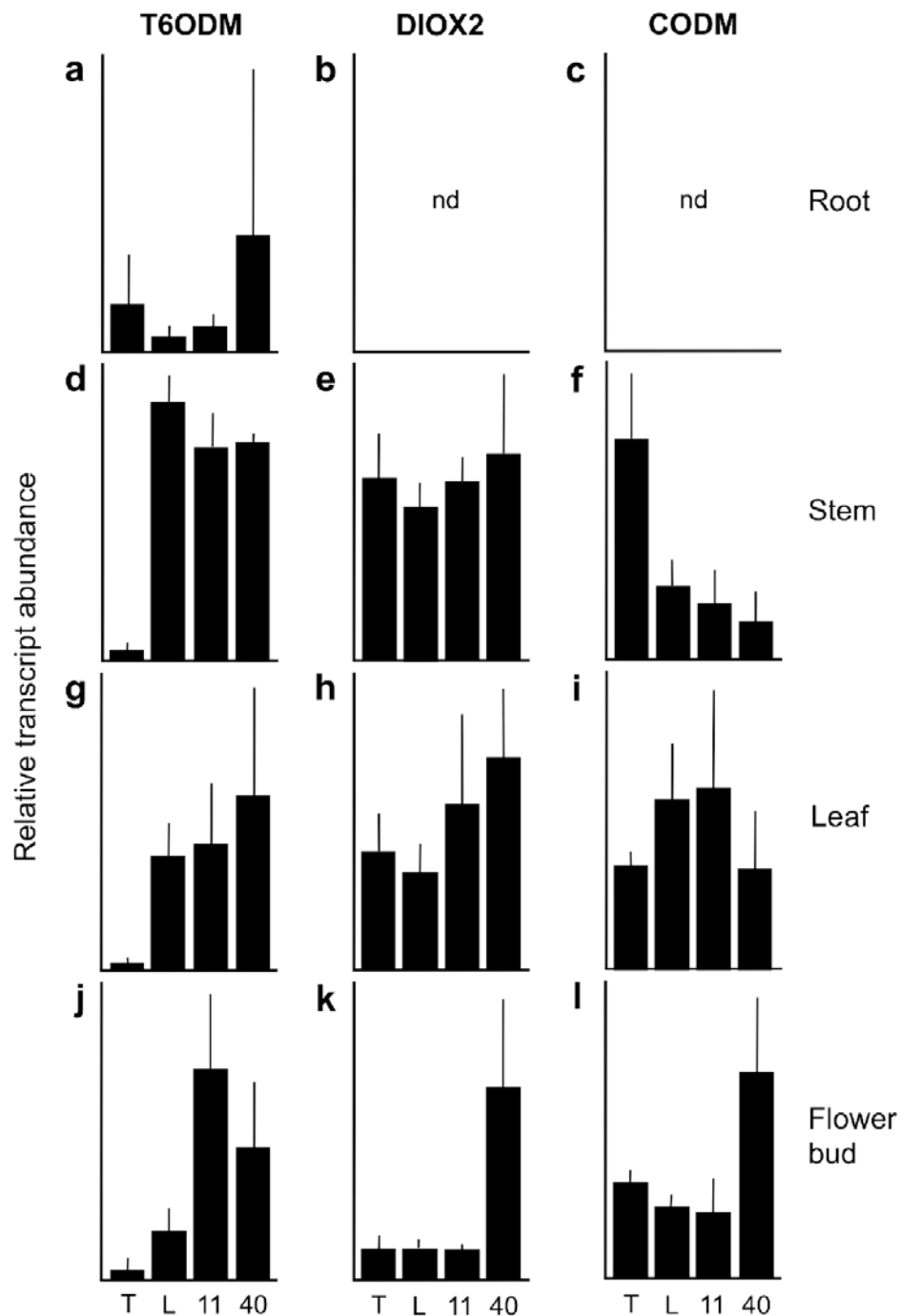
**Supplementary Figure 10. Steady-state enzyme kinetics of purified recombinant thebaine 6-*O*-demethylase (T6ODM, left panels) and codeine *O*-demethylase (CODM, right panels) with varying different substrate concentrations.** Enzyme assays were based on the decarboxylation of [1-<sup>14</sup>C]2-oxoglutarate coupled with the *O*-demethylation of a benzyloquinoline alkaloid co-substrate. The incubation time (45 min), protein concentration (10.0 ng/μl) and other assay parameters were optimized prior to enzyme kinetic analyses. Values represent the mean specific activity ± standard deviation monitored as a function of substrate concentration for three independent replicates. Data was subjected to further analysis using FigP v. 2.98 (BioSoft, Cambridge, UK), generating maximum velocity ( $V_m$ ) and substrate affinity ( $K_m$ ) constants based on Michaelis-Menten kinetics. Curve-fitting for data shown in (a) and (b) revealed moderate substrate inhibition; thus, optimal velocity ( $V_{opt}$ ) and inhibition ( $K_i$ ) constants were also calculated (Supplementary Table 3). Corresponding  $r^2$  values are displayed in the right-hand corners of each panel.



**Supplementary Figure 11. Proposed reaction mechanisms for the 6-*O*-demethylation of thebaine by T6ODM (a) and the 3-*O*-demethylation of codeine by CODM (b).** Identical mechanisms are proposed for the 6-*O*-demethylation of oripavine and the 3-*O*-demethylation of thebaine by T6ODM and CODM, respectively. In all cases, alkyl hydroxylation proceeds through a radical mechanism involving an iron-oxo intermediate, followed by the elimination of formaldehyde. The production of formaldehyde was demonstrated in all cases using the Nash assay<sup>21</sup>. The quantification of formaldehyde release after the incubation of native (closed circles) or denatured (open circles) T6ODM with thebaine (c) or CODM with codeine (d) is shown.



**Supplementary Figure 12. Regions of T6ODM, DIOX2 and CODM cDNAs used to construct virus-induced gene silencing (VIGS) vectors in pTRV2.** Coding regions of each cDNA are shown as thicker line elements, whereas non-coding 5' and 3'-untranslated regions (UTRs) are shown as thinner line elements. The green segment and dotted lines show a region of the T6ODM cDNA that is highly conserved in DIOX2 and CODM, and was used to construct the DIOX-a VIGS vector. The red segments represent unique regions in each cDNA that were used to construct gene-specific VIGS vectors, DIOX-b, DIOX-c and DIOX-d. DNA sequence length is shown in base pairs (bp) with respect to the start codon in each cDNA.



**Supplementary Figure 13. Relative abundance of transcripts encoding thebaine 6-*O*-demethylase (T6ODM), DIOX2 and codeine *O*-demethylase (CODM) in opium poppy plant organs.** Real-time quantitative PCR was used to quantify the relative transcript abundance in roots, stems, leaves and flower buds of opium poppy varieties T, L, 11 and 40. Data were calculated using nine independent trials per plant line (i.e. 3 technical replicates on each of 3 individual plants). Normalization was performed using elongation factor 1a (*elf1a*) as the internal control, and the plant line exhibiting the highest expression level served as the calibrator for each target gene. *DIOX2* and *CODM* transcripts were below detection limits in root (a and c, respectively). Abbreviation: nd, not detected.



**Supplementary Table 1:** Genetic inheritance of the alkaloid phenotype in opium poppy variety T.

Generation	Cross	Phenotype (%T, n=48)
F <sub>1</sub>	♂ <sub>40</sub> x ♀ <sub>T</sub>	0
	♀ <sub>40</sub> x ♂ <sub>T</sub>	0
F <sub>2</sub>	♂ <sub>40</sub> x ♀ <sub>T</sub>	25
	♀ <sub>40</sub> x ♂ <sub>T</sub>	23
	♂ <sub>11</sub> x ♀ <sub>T</sub>	29
	♀ <sub>11</sub> x ♂ <sub>T</sub>	23
Backcross	♂ <sub>40</sub> x [♂ <sub>40</sub> x♀ <sub>T</sub> ]	0
	♀ <sub>40</sub> x [♀ <sub>T</sub> x♂ <sub>40</sub> ]	0
	♀ <sub>T</sub> x [♀ <sub>40</sub> x♂ <sub>T</sub> ]	48
	♂ <sub>T</sub> x [♀ <sub>T</sub> x♂ <sub>40</sub> ]	56

**Supplementary Table 2:** PCR primers used for the assembly of expression vectors and virus-induced gene-silencing constructs, and for real-time quantitative PCR (RT-qPCR) analysis.

**Protein Expression**

Primers used to amplify ORFs for ligation to pQE30

ORF	Forward primer	Reverse primer
<i>DIOX1 (T60DM)</i>	GCGCGGATCCATGGAGAAAGCAAACTT	GCGCCTGCAGCACAAACGCACTTTCGAGA
<i>DIOX2</i>	GCGCGGATCCATGGAGACAGCAAACTT	GCGCCTGCAGAGAGTCAAAAAGCAATGA
<i>DIOX3 (CODM)</i>	GCGCGGATCCATGGAGACACCAATACTT	GCGCCTGCAGGCACCATATGAATTCTTC

**Virus-induced gene silencing**

Primers used in sequence amplification for ligation to TRV2

Sequence	Forward primer	Reverse primer
DIOX-a	GCGCGGATCCCCTTGTCCTCAACCAAAT	GCGCCTCGAGTCCACTTTTAAACAAAGC
DIOX-b	GCGCGGATCCCGACGTGATTGCATGTCA	GCGCCTCGAGCACAAACGCACTTTCGAGA
DIOX-c	GCGCGGATCCTTGATTCGATGAGGATG	GCGCCTCGAGCTTGAGAAAAGTTTTATT
DIOX-d	GCGCGGATCCGTGAGAAAGTGTGAACAT	GCGCCTCGAGCAATCCAATACATTATTT

**RT-qPCR**

Primers used to examine gene-specific transcript abundance

Gene	Forward primer	Reverse primer
<i>DIOX1 (T60DM)</i>	TTGAGGCACAAATGAGAAAATTGA	CACAACGCACTTTCGAGAAATTAC
<i>DIOX2</i>	TGTGAGAAACTGAAGAACACCCAAT	AAGGACTCAAACCACTGAAAGACG
<i>DIOX3 (CODM)</i>	TTGTGCTTAAATTTCTGTGGATGAC	TGATTACATCACTTGACCCAAACAG

**Supplementary Table 3:** Kinetic data for T6ODM and CODM.

Enzyme	Substrate	$K_m$ ( $\mu\text{M}$ )	$K_i$ ( $\mu\text{M}$ )	$V_{\text{max}}$ ( $\text{pkat}$ )	$k_{\text{cat}}$ ( $\text{s}^{-1}$ )	$k_{\text{cat}}/K_m$ ( $\text{s}^{-1} \text{M}^{-1}$ )
T6ODM	Thebaine	20.3 $\pm$ 7.1	518 $\pm$ 237	2.09 $\pm$ 0.33	0.0170 $\pm$ 0.0027	837.1
T6ODM	Oripavine	15.4 $\pm$ 2.7	-	2.35 $\pm$ 0.09	0.0191 $\pm$ 0.0007	1242.6
T6ODM	2-Oxoglutarate	16.4 $\pm$ 5.3	-	1.00 $\pm$ 0.07	0.0081 $\pm$ 0.0006	492.9
CODM	Codeine	20.5 $\pm$ 8.0	642 $\pm$ 409	1.97 $\pm$ 0.35	0.0161 $\pm$ 0.0029	785.4
CODM	Thebaine	41.9 $\pm$ 8.0	-	1.21 $\pm$ 0.06	0.0099 $\pm$ 0.0005	235.2
CODM	2-Oxoglutarate	19.0 $\pm$ 3.3	-	1.35 $\pm$ 0.05	0.0110 $\pm$ 0.0004	578.9

## References

26. Wheeler, D. M. S., Kinstle, T. H. & Rinehart, K. L. J. Mass spectral studies of alkaloids related to morphine. *J. Am. Chem. Soc.* **89**, 4494-4501 (1967).
27. Liscombe, D. K. *et al.* Targeted metabolite and transcript profiling for elucidating enzyme function: Isolation of novel *N*-methyltransferases from three benzyloisoquinoline alkaloid-producing species. *Plant J.* doi: 10.1111/j.1365-313X.2009.03980.x (2009).
28. Ziegler, J., Brandt, W., Geissler, R. & Facchini, P. J. Removal of substrate inhibition and increase in maximal velocity in the short chain dehydrogenase/reductase salutaridine reductase involved in morphine biosynthesis. *J. Biol. Chem.* **284**, 26758-26767 (2009).
29. Chenna, R. *et al.* Multiple sequence alignment with the Clustal series of programs. *Nucleic Acids Res.* **31**, 3497-3500 (2003).
30. Page, R.D. TREEVIEW: an application to display phylogenetic trees on personal computers. *Comput. Appl. Biosci.* **12**, 357-358 (1996).
31. Zulak, K. G. *et al.* Gene transcript and metabolite profiling of elicitor-induced opium poppy cell cultures reveals the coordinate regulation of primary and secondary metabolism. *Planta* **225**, 1085-1106 (2007).
32. Logemann, J., Schell, J. & Willmitzer, L. Improved method for the isolation of RNA from plant tissues. *Anal. Biochem.* **163**, 16-20 (1987).
33. Chirgwin, J. M., Przybyla, A. E., MacDonald, R. J. & Rutter, W. J. Isolation of biologically active ribonucleic acid from sources enriched in ribonuclease. *Biochemistry* **18**, 5294-5299 (1979).
34. Saeed, A. I. *et al.* TM4: a free, open-source system for microarray data management and analysis. *Biotechniques* **34**, 374-378 (2003).
35. Laemmli, U. K. Cleavage of structural proteins during the assembly of the head of bacteriophage T4. *Nature* **227**, 680-685 (1970).
36. Raith K. *et al.* Electrospray tandem mass spectrometric investigations of morphinans. *J. Am. Soc. Mass Spectrom.* **14**, 1262-1269 (2003).
37. Schmidt, J., Boettcher, C., Kuhnt, C., Kutchan, T.M., Zenk, M.H. Poppy alkaloid profiling by electrospray tandem mass spectrometry and electrospray FT-ICR mass spectrometry after [ring-<sup>13</sup>C<sub>6</sub>]-tyramine feeding. *Phytochemistry* **68**, 189-202 (2007).
38. Dinesh-Kumar, S. P. *et al.* Virus-induced gene silencing. *Methods Mol. Biol.* **236**, 287-294 (2003).
39. Liu, Y. L., Schiff, M., Marathe, R. & Dinesh-Kumar, S. P. Tobacco Rar1, *EDS1* and *NPR1/NIM1* like genes are required for *N*-mediated resistance to tobacco mosaic virus. *Plant J.* **30**, 415-429 (2002).
40. Hileman, L.C., Drea, S., de Martino, G., Litt, A. & Irish, V. Virus-induced gene silencing is an effective tool for assaying gene function in the basal eudicot species *Papaver somniferum* (opium poppy). *Plant J.* **44**, 334-341 (2005).

41. Livak, K. J. & Schmittgen, T. D. Analysis of relative gene expression data using real-time quantitative PCR and the  $2^{-\Delta\Delta C_t}$  method. *Methods* **25**, 402–408 (2001).
42. Fisinger, U., Grobe, N. & Zenk, M.H. Thebaine synthase: a new enzyme in the morphine pathway in *Papaver somniferum*. *Nat. Prod. Commun.* **2**, 249-253 (2007).
43. Lenz, R. & Zenk, M.H. Purification and properties of codeinone reductase (NADPH) from *Papaver somniferum* cell cultures and differentiated plants. *Eur. J. Biochem.* **233**, 132-139 (1995).